

100 Years of the Radon Transform

**Travel Time Tomography and generalized
Radon Transforms**

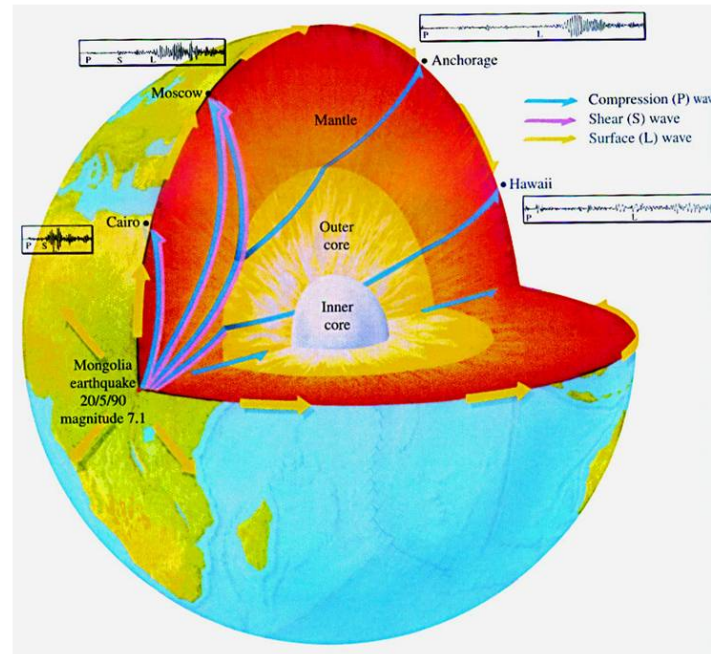
Gunther Uhlmann

University of Washington, HKUST
and U. Helsinki

Linz, Austria, March 29, 2017

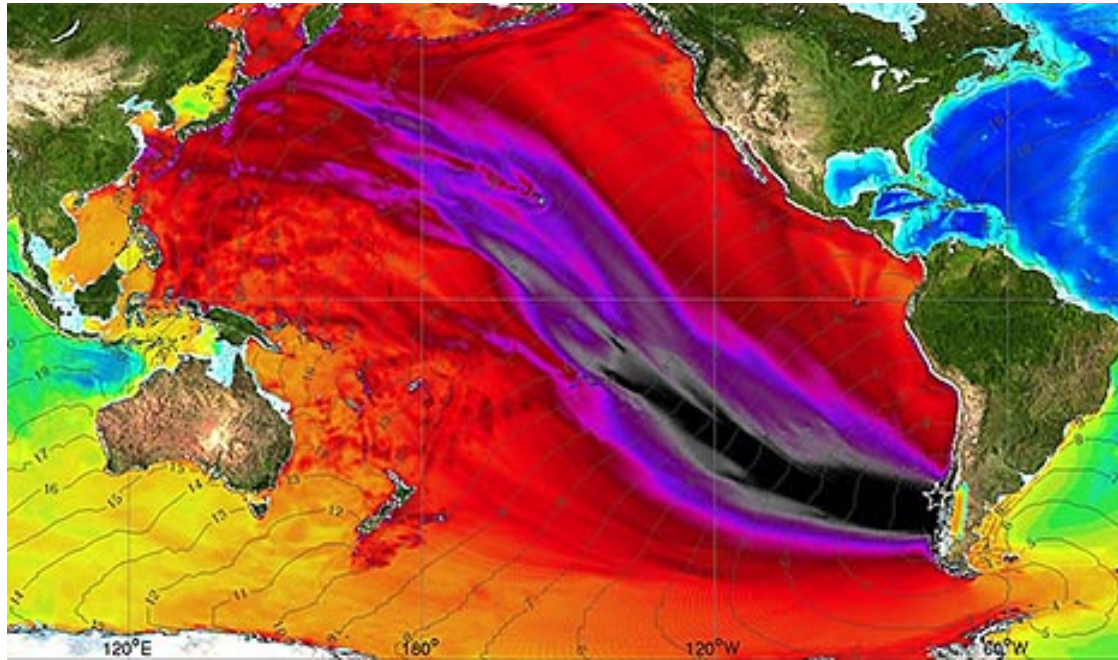
Travel Time Tomography (Transmission)

Global Seismology



Inverse Problem: Determine inner structure of Earth by measuring travel time of seismic waves.

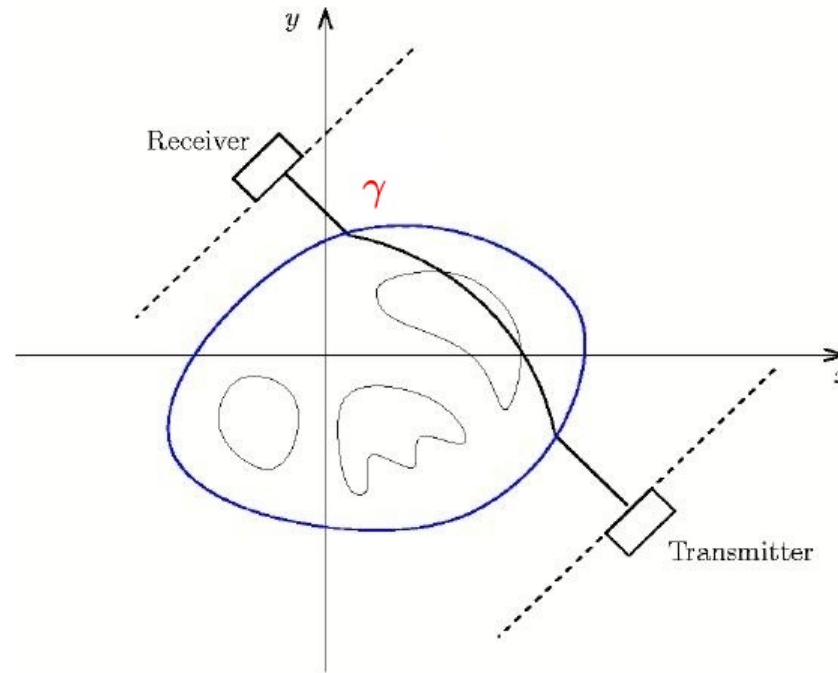
Tsunami of 1960 Chilean Earthquake



Black represents the largest waves, decreasing in height through purple, dark red, orange and on down to yellow. In 1960 a tongue of massive waves spread across the Pacific, with big ones throughout the region.

Human Body Seismology

ULTRASOUND TRANSMISSION TOMOGRAPHY(UTT)

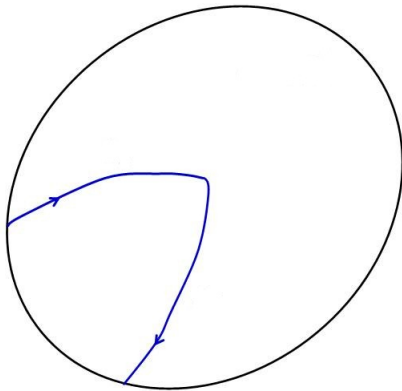


$$T = \int_{\gamma} \frac{1}{c(x)} ds = \text{Travel Time (Time of Flight)}.$$

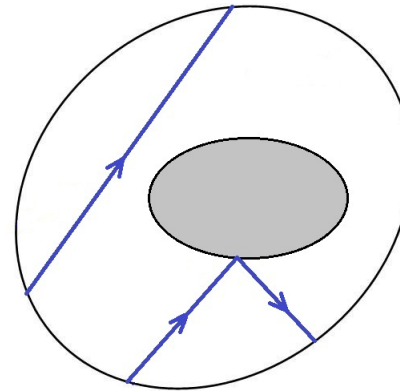
REFLECTION TOMOGRAPHY

Scattering

Points in medium

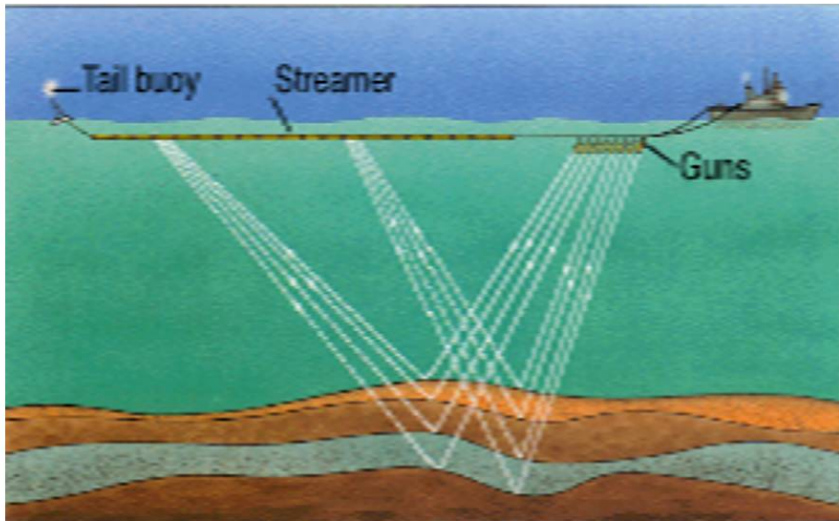


Obstacle



REFLECTION TOMOGRAPHY

Oil Exploration

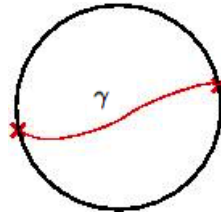


Ultrasound



TRAVELTIME TOMOGRAPHY (Transmission)

Motivation: Determine inner structure of Earth by measuring travel times of seismic waves



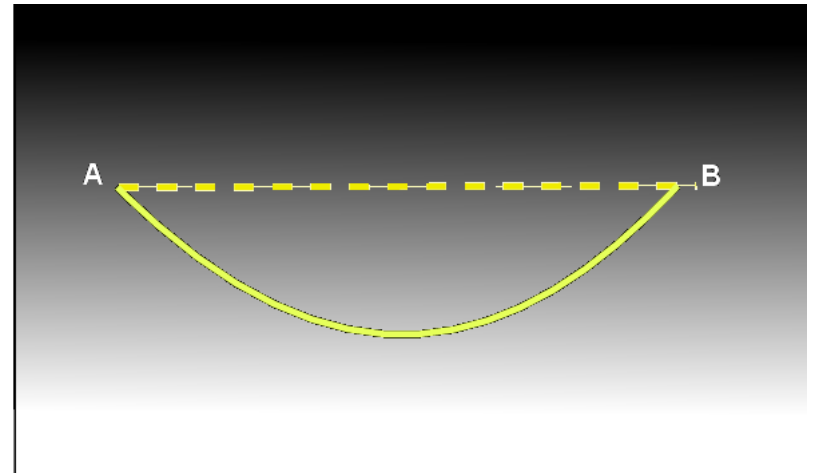
Herglotz (1905), Wiechert-Zoeppritz (1907)

Sound speed $c(r)$, $r = |x|$

$$\frac{d}{dr} \left(\frac{r}{c(r)} \right) > 0$$

$T = \int_{\gamma} \frac{1}{c(r)}$. What are the curves of propagation γ ?

Ray Theory of Light: Fermat's principle



Fermat's principle. Light takes the shortest optical path from A to B (solid line) which is not a straight line (dotted line) in general. The optical path length is measured in terms of the refractive index n integrated along the trajectory. The greylevel of the background indicates the refractive index; darker tones correspond to higher refractive indices.

The curves are **geodesics** of a metric.

$$ds^2 = \frac{1}{c^2(r)} dx^2$$

More generally $ds^2 = \frac{1}{c^2(x)} dx^2$

Velocity $v(x, \xi) = c(x)$, $|\xi| = 1$ (isotropic)

Anisotropic case

$$ds^2 = \sum_{i,j=1}^n g_{ij}(x) dx_i dx_j$$

$g = (g_{ij})$ is a positive definite symmetric matrix

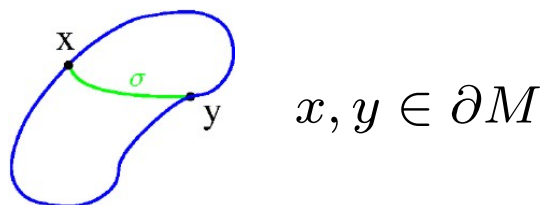
Velocity $v(x, \xi) = \sqrt{\sum_{i,j=1}^n g^{ij}(x) \xi_i \xi_j}$, $|\xi| = 1$

$$g^{ij} = (g_{ij})^{-1}$$

The information is encoded in the
boundary distance function

More general set-up

(M, g) a Riemannian manifold with boundary (compact) $g = (g_{ij})$



$$d_g(x, y) = \inf_{\substack{\sigma(0)=x \\ \sigma(1)=y}} L(\sigma)$$

$L(\sigma) =$ length of curve σ

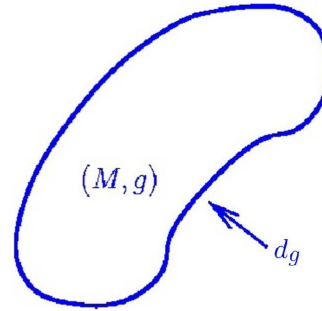
$$L(\sigma) = \int_0^1 \sqrt{\sum_{i,j=1}^n g_{ij}(\sigma(t)) \frac{d\sigma_i}{dt} \frac{d\sigma_j}{dt}} dt$$

Inverse problem

Determine g knowing $d_g(x, y)$ $x, y \in \partial M$

ANOTHER MOTIVATION (STRING THEORY)

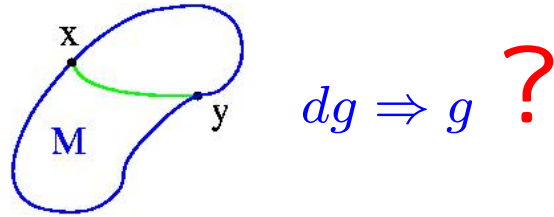
HOLOGRAPHY



Inverse problem: Can we recover (M, g) (bulk) from boundary distance function ?

M. Parrati and R. Rabadan, Boundary rigidity and holography, JHEP 01 (2004) 034

B. Czech, L. Lamprou, S. McCandlish and J. Sully, Integral geometry and holography, JHEP 10 (2015) 175



(Boundary rigidity problem)

Answer NO

$\psi : M \rightarrow M$ diffeomorphism

$$\psi|_{\partial M} = \text{Identity}$$

$$d\psi^*g = dg$$

$$\psi^*g = \left(D\psi \circ g \circ (D\psi)^T \right) \circ \psi$$

$$L_g(\sigma) = \int_0^1 \sqrt{\sum_{i,j=1}^n g_{ij}(\sigma(t)) \frac{d\sigma_i}{dt} \frac{d\sigma_j}{dt}} dt$$

$\tilde{\sigma} = \psi \circ \sigma$

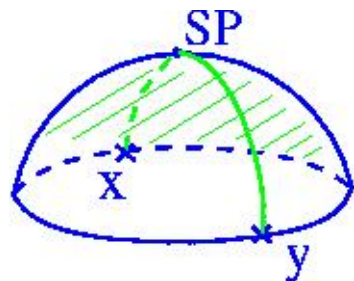
$L_{\psi^*g}(\tilde{\sigma}) = L_g(\sigma)$

$$d_{\psi^*g} = d_g$$

Only obstruction to determining g from d_g ? No



$$d_g(x_0, \partial M) > \sup_{x,y \in \partial M} d_g(x, y)$$



Can change metric near SP

Def (M, g) is **boundary rigid** if (M, \tilde{g}) satisfies $d_{\tilde{g}} = d_g$. Then $\exists \psi : M \rightarrow M$ diffeomorphism, $\psi|_{\partial M} = \text{Identity}$, so that

$$\tilde{g} = \psi^* g$$

Need an a-priori condition for (M, g) to be boundary rigid.

One such condition is that (M, g) is **simple**

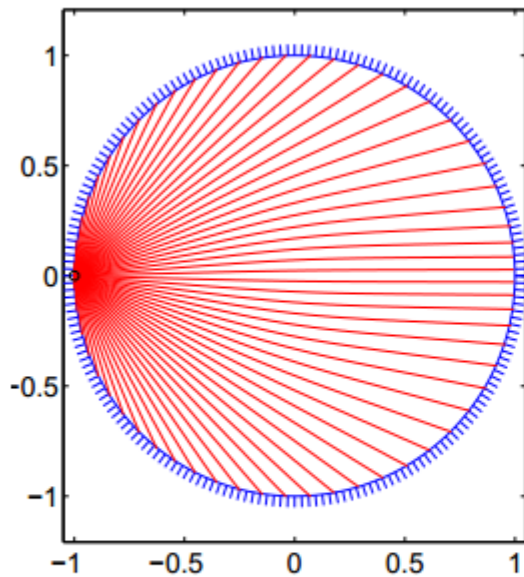
DEF (M, g) is **simple** if given two points $x, y \in \partial M$, $\exists!$ geodesic joining x and y and ∂M is strictly convex

CONJECTURE

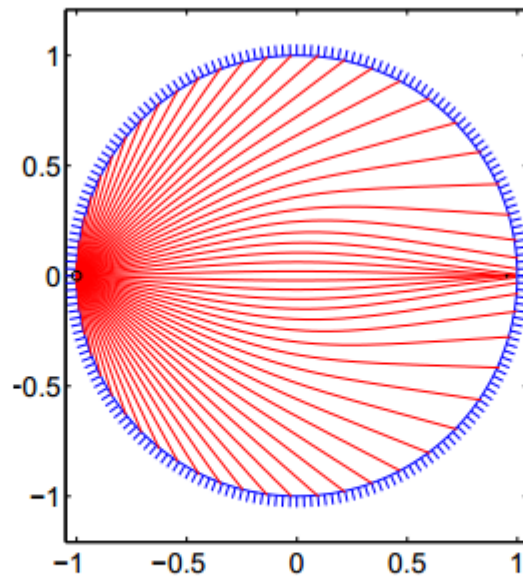
(M, g) is **simple** then (M, g) is boundary rigid, that is d_g determines g up to the natural obstruction. ($d_{\psi^*g} = d_g$)

(Conjecture posed by R. Michel, 1981)

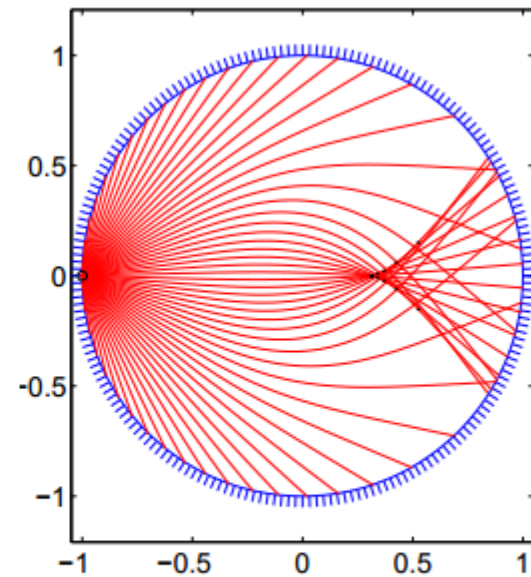
Metrics Satisfying the Herglotz condition



$k = 0.20$ (simple)



$k = 0.49$ (non-simple)



$k = 1.23$ (non-simple)

$$g_k(r) = \exp \left(k \exp \left(-\frac{r^2}{2\sigma^2} \right) \right), \quad 0 \leq r \leq 1, \quad \sigma \text{ fixed}$$

Francois Monard: SIAM J. Imaging Sciences (2014)

Results in the Isotropic Case

$$d_{\beta g} = d_g \implies \beta = 1?$$

Theorem (Mukhometov, Mukhometov-Romanov, Beylkin, Gerver-Nadirashvili, ...)

YES for simple manifolds. Also stability.

The sound speed case corresponds to $g = \frac{1}{c^2}e$ with e the identity.

Results (M, g) simple

- R. Michel (1981) Compact subdomains of \mathbb{R}^2 or \mathbb{H}^2 or the open round hemisphere
- Gromov (1983) Compact subdomains of \mathbb{R}^n
- Besson-Courtois-Gallot (1995) Compact subdomains of **negatively curved symmetric spaces**

(All examples above have constant curvature)

- $\left\{ \begin{array}{l} \text{Stefanov-U (1998)} \\ \text{Lassas-Sharafutdinov-U} \\ \text{(2003)} \\ \text{Burago-Ivanov (2010)} \end{array} \right\} \quad dg = dg_0, \quad g_0 \text{ close to} \\ \text{Euclidean}$

$$n = 2$$

- Otal and Croke (1990) $K_g < 0$

THEOREM(Pestov-U, 2005)

Two dimensional Riemannian manifolds with boundary which are simple are boundary rigid ($d_g \Rightarrow g$ up to natural obstruction)

Theorem ($n \geq 3$) (Stefanov-U, 2005)

(M, g_i) simple $i = 1, 2$, g_i close to $g_0 \in \mathcal{L}$ where \mathcal{L} is a generic set of simple metrics in $C^k(M)$. Then

$d_{g_1} = d_{g_2} \Rightarrow \exists \psi : M \rightarrow M$ diffeomorphism,

$\psi|_{\partial M} = \text{Identity}$, so that $g_1 = \psi^* g_2$

Also **Stability**.

Remark

If M is an open set of \mathbb{R}^n , \mathcal{L} contains all simple and real-analytic metrics in $C^k(M)$.

Geodesics in Phase Space

$g = (g_{ij}(x))$ symmetric, positive definite

Hamiltonian is given by

$$H_g(x, \xi) = \frac{1}{2} \left(\sum_{i,j=1}^n g^{ij}(x) \xi_i \xi_j - 1 \right) \quad g^{-1} = (g^{ij}(x))$$

$X_g(s, X^0) = (x_g(s, X^0), \xi_g(s, X^0))$ be bicharacteristics,

sol. of
$$\frac{dx}{ds} = \frac{\partial H_g}{\partial \xi}, \quad \frac{d\xi}{ds} = -\frac{\partial H_g}{\partial x}$$

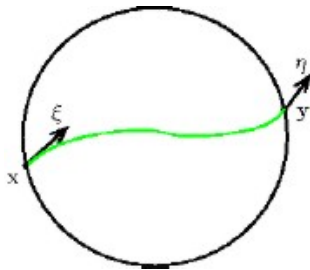
$x(0) = x^0, \xi(0) = \xi^0, X^0 = (x^0, \xi^0)$, where $\xi^0 \in \mathcal{S}_g^{n-1}(x^0)$
 $\mathcal{S}_g^{n-1}(x) = \{ \xi \in \mathbb{R}^n; H_g(x, \xi) = 0 \}.$

Geodesics Projections in x : $x(s)$.

Scattering Relation

d_g only measures first arrival times of waves.

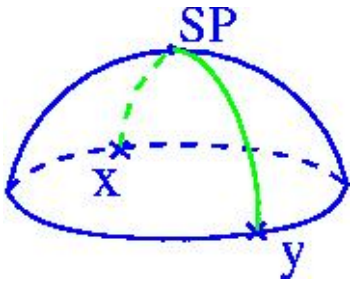
We need to look at behavior of **all** geodesics



$$\|\xi\|_g = \|\eta\|_g = 1$$

$\alpha_g(x, \xi) = (y, \eta)$, α_g is SCATTERING RELATION

If we know **direction** and **point** of entrance of geodesic then we know its **direction** and **point** of exit.



Scattering relation follows **all** geodesics.

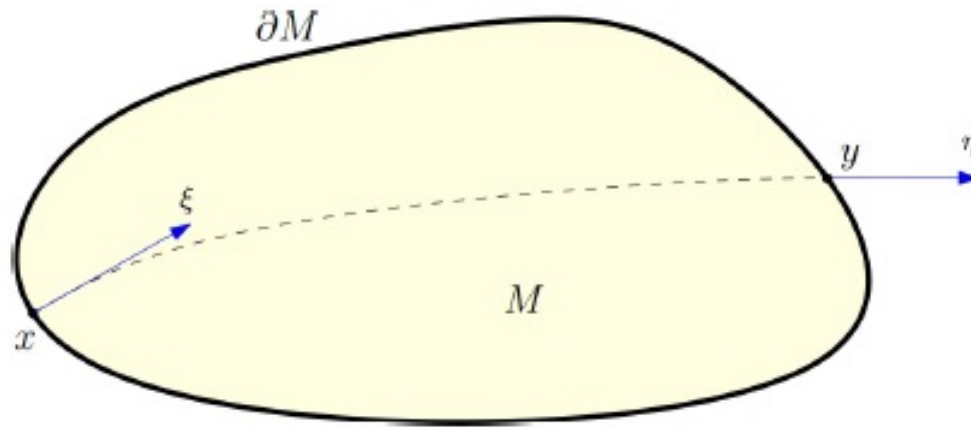
Conjecture Assume (M, g) non-trapping. Then α_g determines g up to natural obstruction.

(Pestov-U, 2005) $n = 2$ Connection between α_g and Λ_g (Dirichlet-to-Neumann map)

(M, g) simple then $d_g \Leftrightarrow \alpha_g$

Lens Rigidity

Define the scattering relation α_g and the length (travel time) function ℓ :



$$\alpha_g : (x, \xi) \rightarrow (y, \eta), \quad \ell(x, \xi) \rightarrow [0, \infty].$$

Diffeomorphisms preserving ∂M pointwise do not change L, ℓ !

Lens rigidity: *Do α_g, ℓ determine g uniquely, up to isometry?*

Lens rigidity: *Do α_g, ℓ determine g uniquely, up to isometry?*

No, There are counterexamples for trapping manifolds (Croke-Kleiner).

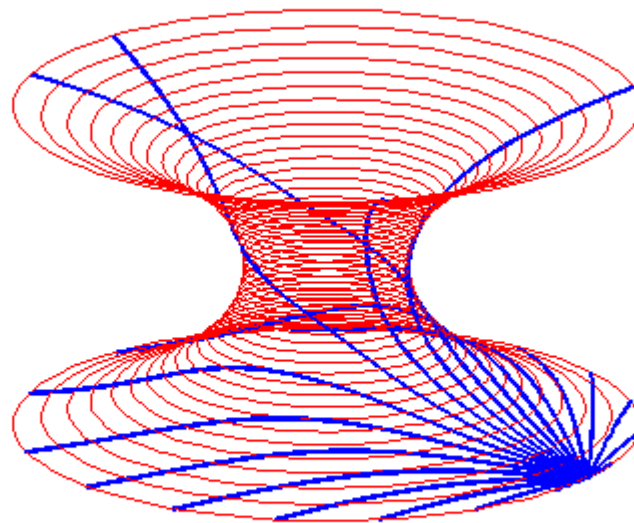
The **lens rigidity** problem and the **boundary rigidity** one are equivalent for **simple metrics**! This is also true locally, near a point p where ∂M is strictly convex.

For **non-simple metrics** (caustics and/or non-convex boundary), **lens rigidity** is the right problem to study.

Some results: local generic rigidity near a class of non-simple metrics (Stefanov-U, 2009), lens rigidity for real-analytic metrics satisfying a mild condition (Vargo, 2010), the torus is lens rigid (Croke 2014), stability estimates for a class of non-simple metrics (Bao-Zhang 2014), Stefanov-U-Vasy, 2013 (foliation condition, conformal case); Guillarmou, 2015 (hyperbolic trapping), Stefanov-U-Vasy, 2017 (foliation condition, general case).

Theorem (C. Guillarmou 2015). Let (M, g) be a surface with strictly convex boundary and [hyperbolic trapping](#) and no conjugate points. Then [lens](#) data determines the metric up to a conformal factor.

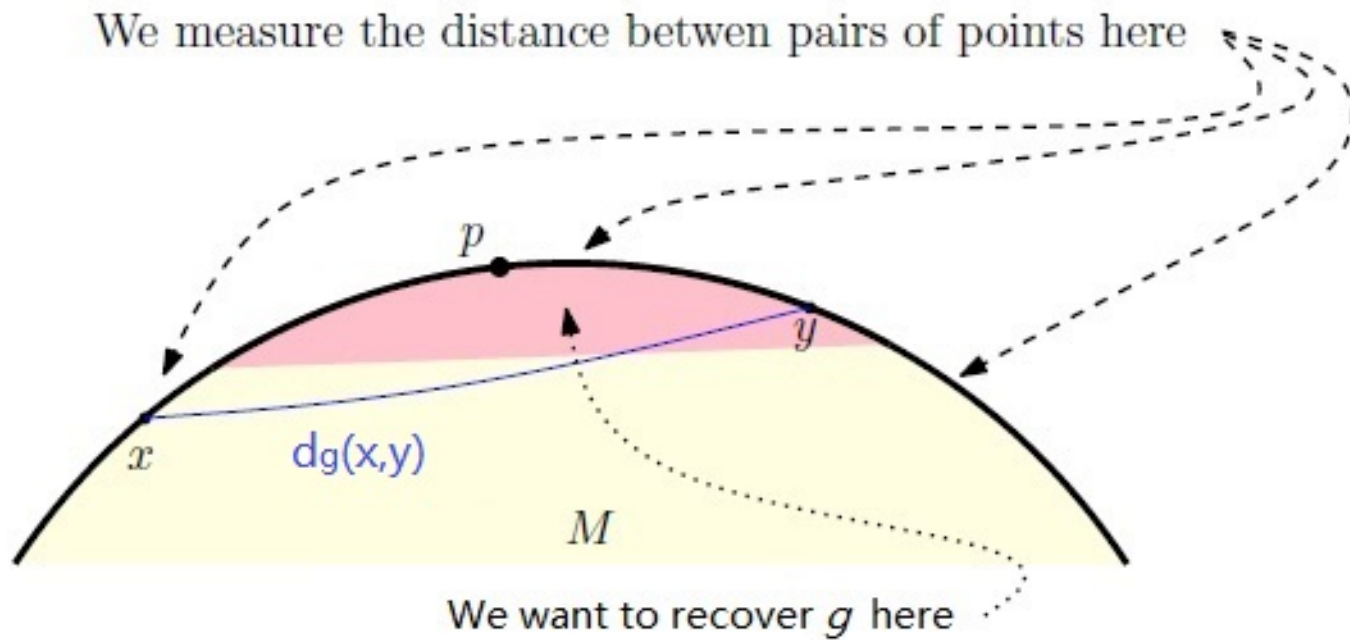
[Dynamical Systems and Microlocal Analysis](#) (Faure-Sjöstrand, Dyatlov-Zworski, Dyatlov-Guillarmou)



(Picture by F. Monard)

Partial Data: General Case

Boundary Rigidity with partial data: Does d_g , known on $\partial M \times \partial M$ near some p , determine g near p up to isometry?



Theorem (Stefanov-U-Vasy, 2017). Let $\dim M \geq 3$. If ∂M is strictly convex near p for g and \tilde{g} , and $d_g = d_{\tilde{g}}$ near (p, p) , then $g = \tilde{g}$ up to isometry near p .

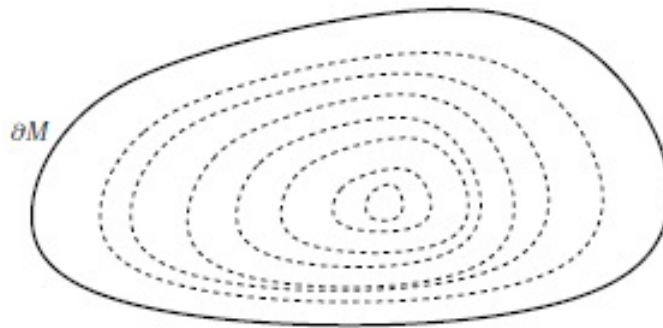
Also **stability** and **reconstruction**.

The only results so far of similar nature is for **real analytic** metrics (Lassas-Sharafutdinov-U, 2003). We can recover the whole **jet** of the metric at ∂M and then use analytic continuation.

Global result under the foliation condition

We could use a layer stripping argument to get deeper and deeper in M and prove that one can determine g (up to isometry) in the whole M .

Foliation condition: M is foliated by strictly convex hypersurfaces if, up to a nowhere dense set, $M = \cup_{t \in [0, T)} \Sigma_t$, where Σ_t is a smooth family of strictly convex hypersurfaces and $\Sigma_0 = \partial M$.



A more general condition: several families, starting from outside M .

Global result under the foliation condition

Theorem (Stefanov-U-Vasy, 2016). Let $\dim M \geq 3$, let $\tilde{g} = \beta g$ with $\beta > 0$ smooth on M , let ∂M be strictly convex with respect to both g and \tilde{g} . Assume that M can be foliated by strictly convex hypersurfaces for g . Then if $\alpha_g = \alpha_{\tilde{g}}, l = \tilde{l}$ we have $g = \tilde{g}$ in M .

Examples: The foliation condition is satisfied for strictly convex manifolds of non-negative sectional curvature, simply connected manifolds with non-positive sectional curvature and simply connected manifolds with no focal points.

Foliation condition is an analog of the Herglotz, Wieckert-Zoeppritz condition for non radial speeds.

Example: Herglotz and Wiechert & Zoeppritz showed that one can determine a radial speed $c(r)$ in the ball $B(0, 1)$ satisfying

$$\frac{d}{dr} \frac{r}{c(r)} > 0.$$

The uniqueness is in the class of radial speeds.

One can check directly that their condition is equivalent to the following one: the Euclidean spheres $\{|x| = t\}$, $t \leq 1$ are strictly convex for $c^{-2}dx^2$ as well. Then $B(0, 1)$ satisfies the foliation condition. Therefore, if $\tilde{c}(x)$ is another speed, not necessarily radial, with the same lens relation, equal to c on the boundary, then $c = \tilde{c}$. There could be conjugate points.

Therefore, speeds satisfying the Herglotz and Wiechert & Zoeppritz condition are conformally lens rigid.

Global result in the general case

Theorem (Stefanov-U-Vasy, 2017). Let (M, g) be a compact n -dimensional Riemannian manifold, $n \geq 3$, with strictly convex boundary so that there exists a strictly convex function f on M with $\{f = 0\} = \partial M$. Let \tilde{g} be another Riemannian metric on M , and assume that ∂M is strictly convex w.r.t. \tilde{g} as well. If g and \tilde{g} have the same lens relations, then there exists a diffeomorphism ψ on M fixing ∂M pointwise such that $g = \psi^* \tilde{g}$.

Examples: This condition is satisfied for strictly convex manifolds of non-negative sectional curvature, simply connected manifolds with non-positive sectional curvature and simply connected manifolds with no focal points.

New Results on Boundary Rigidity

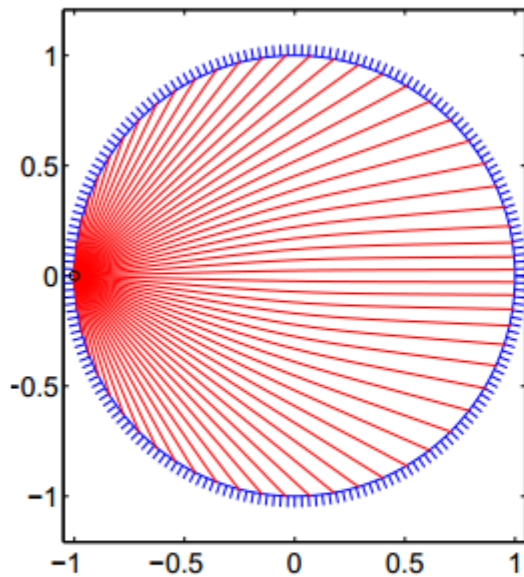
The **Boundary Rigidity** problem is to recover g from d_g .

Corollary (New result on boundary rigidity). Strictly convex, simply connected manifolds with **no focal points** are **boundary rigid**.

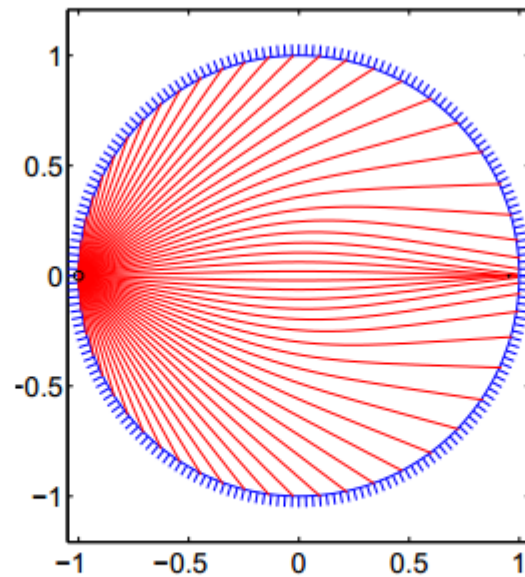
Strictly convex, simply connected manifolds with no focal points are **simple**.

Question: Do **simple** manifolds satisfy the **foliation condition**?

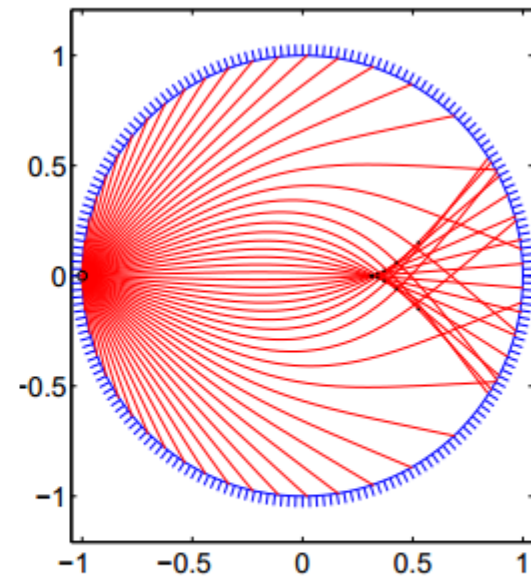
Metrics Satisfying the Herglotz condition



$k = 0.20$ (simple)



$k = 0.49$ (non-simple)



$k = 1.23$ (non-simple)

$$g_k(r) = \exp \left(k \exp \left(-\frac{r^2}{2\sigma^2} \right) \right), \quad 0 \leq r \leq 1, \quad \sigma \text{ fixed}$$

Francois Monard: SIAM J. Imaging Sciences (2014)

Elasticity

The isotropic elastic equation is given by

$$(\partial_t^2 - E)u = 0,$$

where $u = (u_1, u_2, u_3)$, and

$$(Eu)_i = \rho^{-1} \left(\partial_i \lambda \nabla \cdot u + \sum_j \partial_j \mu (\partial_j u_i + \partial_i u_j) \right),$$

where $\lambda > 0$ and $\mu > 0$ are the Lamé parameters and $\rho > 0$ is the density.

We want to recover λ , μ and ρ from the DN map

$$\Lambda f = \sum_j \sigma_{ij}(u) \nu_j,$$

where ν is the outer normal and $\sigma_{ij}(u) = \lambda \nabla \cdot u \delta_{ij} + \mu (\partial_j u_i + \partial_i u_j)$ is the stress tensor.

The speed of **P-waves** is given by

$$c_p = \sqrt{(\lambda + 2\mu)/\rho}$$

and the speed of **S-waves** is given by

$$c_s = \sqrt{\mu/\rho}.$$

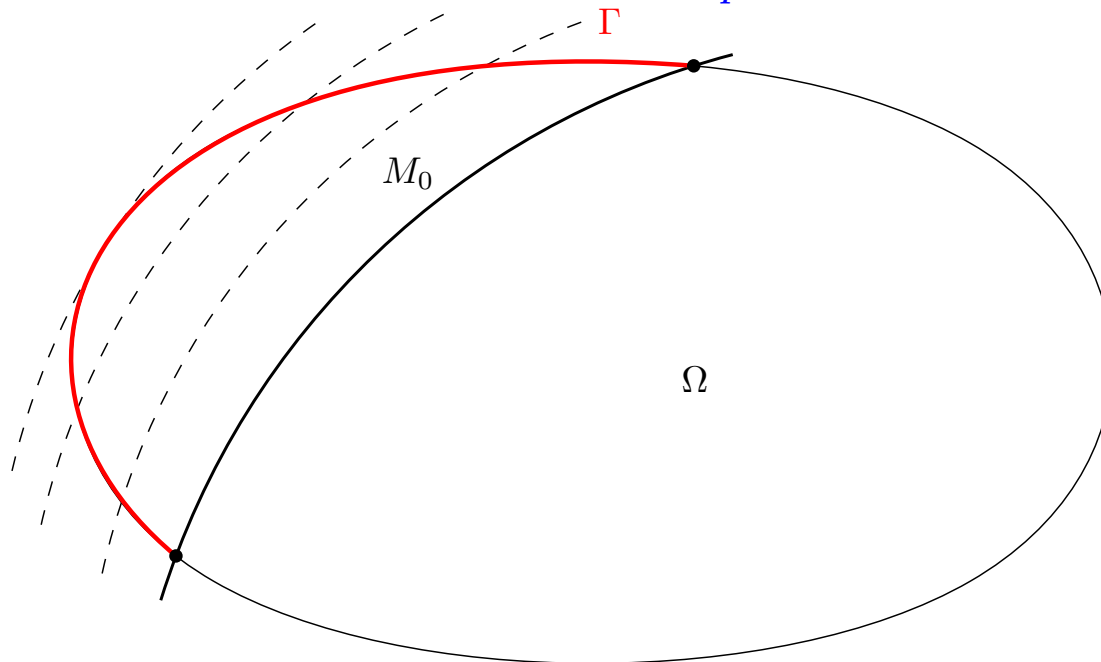
Rachelle has shown that one can recover the boundary jets and the coefficients inside if both speeds are **simple**. The proof of the later uses the boundary rigidity results for $c_p^{-2}dx^2$ and $c_s^{-2}dx^2$ and the inversion of the geodesic ray transform.

Unique continuation holds but the boundary control method does not work. The **local** problem was open.

Theorem (Stefanov-U-Vasy, 2017). Let $\Sigma_q, q \in [0, 1]$ be a strictly convex foliation w.r.t. c_p , and let $\Gamma \subset \partial M$ be defined as $\Gamma = \cup_{q \in [0, 1]} (\partial M \cap \Sigma_q)$.

Then c_p is uniquely determined in the compact set foliated by the foliation by knowledge of Λ on $(0, T) \times \Gamma$ if T is greater than the length of all geodesics, in the metric $c_p^{-2} dx^2$, in $\bar{\Omega}$ having the property that each one is tangent to some Σ_q .

The same statement remains true for c_p replaced by c_s .



In particular, this solves the **local** problem in seismology with local measurements. The foliation condition is satisfied when the two speeds increase with depth, which is true for the actual c_p and c_s according to the popular Preliminary Reference Earth Model (PERM).

To prove the theorem, we show that we can recover the **lens relations** related to both speeds from Λ ; and then apply the local rigidity result for speeds. This approach implies **stability and reconstruction**, as well.



The shaded region is where we can recover the speed if the speed increases with depth.

Inversion of X-ray Transform (Radon 1917)

- $I f(x, \theta) = \int f(x + t\theta) dt, \quad |\theta| = 1$

- $(-\Delta)^{1/2} I^* I f = c f, \quad c \neq 0$

- $(-\Delta)^{-1/2} f = \int \frac{f(y)}{|x - y|^{n-1}} dy$

$I^* I$ is an elliptic pseudodifferential operator of order -1.

Inversion of X-ray Transform

(M, g) simple

$$If(x, \xi) = \int_0^{\tau(x, \xi)} f(\gamma(x, t, \xi)) dt$$

$$\xi \in S_x M = \{\xi \in T_x M : |\xi| = 1\}$$

where $\gamma(x, t, \xi)$ is the geodesic starting from x in direction ξ , $\tau(x, \xi)$ is the exit time.

Theorem (Guillemin 1975, Stefanov-U, 2004). (M, g) simple. Then I^*I is an elliptic pseudodifferential operator of order -1.

Idea of the proof in isotropic case

The proof is based on two main ideas.

First, we use the approach in a recent paper by U-Vasy (2012) on the linear integral geometry problem.

Second, we convert the non-linear boundary rigidity problem to a “pseudo-linear” one. Straightforward linearization, which works for the problem with full data, fails here.

First Idea: The Linear Problem

Let (M, g) be compact with smooth boundary. Linearizing $g \mapsto d_g$ in a fixed conformal class leads to the *ray transform*

$$If(x, \xi) = \int_0^{\tau(x, \xi)} f(\gamma(t, x, \xi)) dt$$

where $x \in \partial M$ and $\xi \in S_x M = \{\xi \in T_x M ; |\xi| = 1\}$.

Here $\gamma(t, x, \xi)$ is the geodesic starting from point x in direction ξ , and $\tau(x, \xi)$ is the time when γ exits M . We assume that (M, g) is *nontrapping*, i.e. τ is always finite.

First Idea: The Linear Problem

U-Vasy result: Consider the inversion of the geodesic ray transform

$$If(\gamma) = \int f(\gamma(s)) ds$$

known for geodesics intersecting some neighborhood of $p \in \partial M$ (where ∂M is strictly convex) “almost tangentially”. It is proven that those integrals determine f near p uniquely. It is a [Helgason](#) support type of theorem for non-analytic curves! This was extended recently by [H. Zhou](#) for arbitrary curves (∂M must be strictly convex w.r.t. them) and non-vanishing weights.

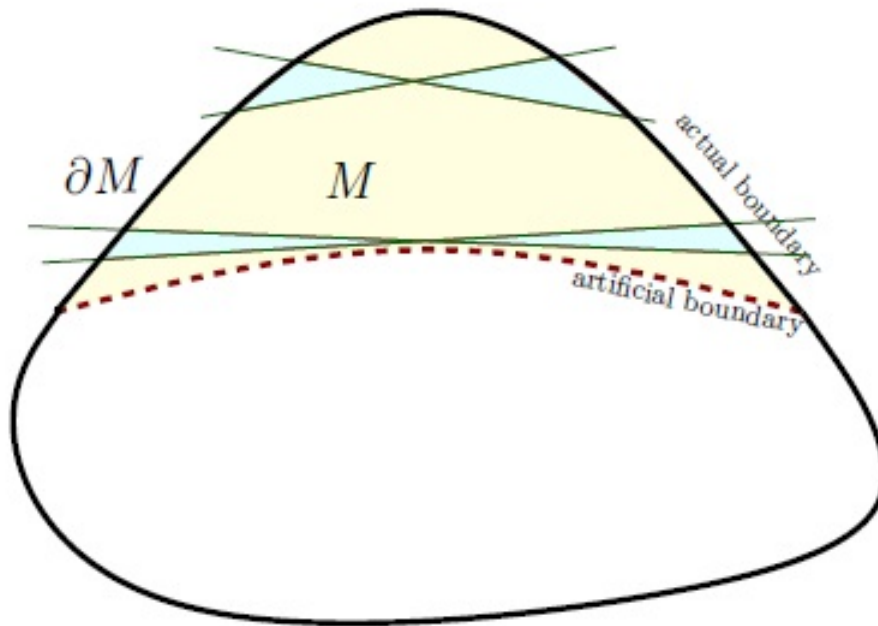
The main idea in U-Vasy is the following:

Introduce an artificial, still strictly convex boundary near p which cuts a small subdomain near p . Then use Melrose's scattering calculus to show that the I , composed with a suitable "back-projection" is elliptic in that calculus. Since the subdomain is small, it would be invertible as well.

Consider

$$Pf(z) := I^* \chi I f(z) = \int_{S_z M} x^{-2} \chi I f(\gamma_{z,v}) dv,$$

where χ is a smooth cutoff sketched below (angle $\sim x$), and x is the distance to the artificial boundary.



Inversion of local geodesic transform

$$Pf(z) := I^* \chi I f(z) = \int_{S_z M} x^{-2} \chi I f(\gamma_{z,v}) dv,$$

Main result: P is an **elliptic** pseudodifferential operator in Melrose's scattering calculus.

There exists A such that $AP = Identity + R$

This is Fredholm and **R has a small norm** in a neighborhood of p .
Therefore invertible near p .

Some results for inverse geodesic X-ray transform

(E. Chung - U, 2017)

- We take spherical domain and the following sound speed

$$c(x, y, z) = 1 + (0.3) \cos \left(\sqrt{(x - 0.5)^2 + (y - 0.5)^2 + (z - 0.5)^2} \right)$$

- We test the method with the following functions

$$f_1 = 0.01 + \sin \left(2\pi(x + y + z)/10 \right),$$

$$f_2 = 0.01 + \sin \left(2\pi(x + y)/10 \right) + \cos \left(2\pi z/20 \right),$$

$$f_3 = x + y^2 + z^2/2,$$

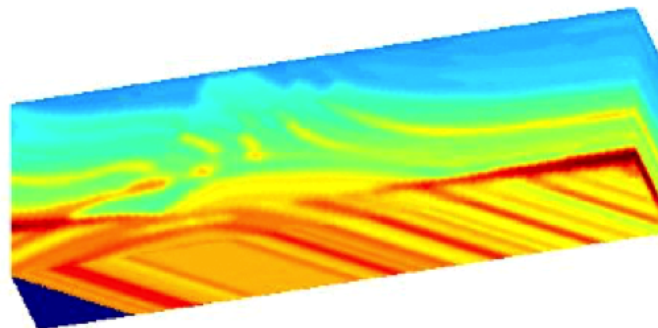
$$f_4 = 1 + 6x + 4y + 9z + \sin \left(2\pi(x + z) \right) + \cos \left(2\pi y \right)$$

$$f_5 = x + e^{y+z/2}.$$

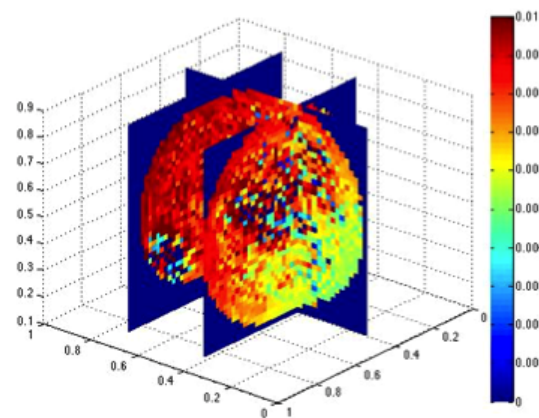
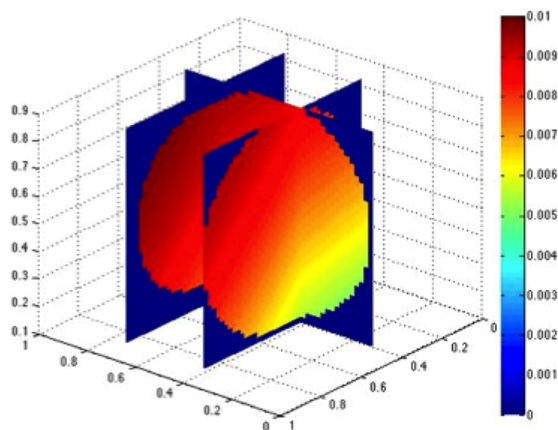
- Relative errors for using up to 4 terms in the Neumann series

relative error	f_1	f_2	f_3	f_4	f_5
n=0	37.1%	37.08%	37.13%	37.27%	37.25%
n=1	15.74 %	15.63%	15.81%	16.2%	16.32 %
n=2	8.92%	8.65%	9.09%	9.98%	10.28%
n=3	6.99%	6.55%	7.26%	8.61%	9.02%

- We test the method using a spherical section of the [Marmousi model](#)



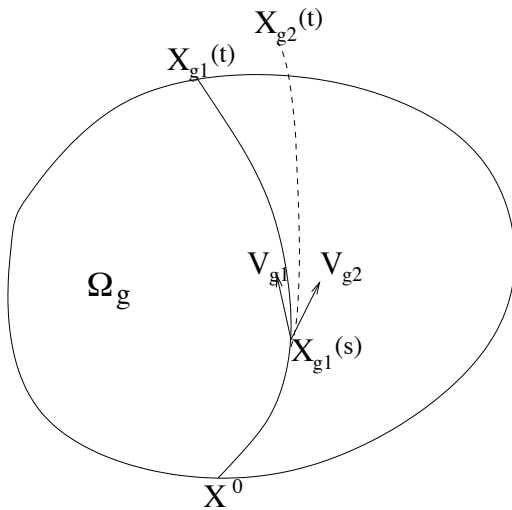
- Results



	$n = 0$	$n = 1$	$n = 2$	$n = 3$
relative error	40.92%	19.89%	14.48%	14.20%
relative error with 5% noisy data	42.15%	22.33%	17.47%	17.12%

Second Step: Reduction to Pseudolinear Problem

Identity (Stefanov-U, 1998)



$$T = d_{g_1},$$

$$F(s) = X_{g_2}(T - s, X_{g_1}(s, X^0)),$$

$$F(0) = X_{g_2}(T, X^0), \quad F(T) = X_{g_1}(T, X^0),$$

$$\int_0^T F'(s) ds = X_{g_1}(T, X^0) - X_{g_2}(T, X^0)$$

$$\int_0^T \frac{\partial X_{g_2}}{\partial X^0}(T - s, X_{g_1}(s, X^0)) (V_{g_1} - V_{g_2}) \Big|_{X_{g_1}(s, X^0)} dS$$

$$= X_{g_1}(T, X^0) - X_{g_2}(T, X^0)$$

Identity (Stefanov-U, 1998)

$$\int_0^T \frac{\partial X_{g_2}}{\partial X^0} (T - s, X_{g_1}(s, X^0)) (V_{g_1} - V_{g_2}) \Big|_{X_{g_1}(s, X^0)} dS \\ = X_{g_1}(T, X^0) - X_{g_2}(T, X^0)$$

$$V_{g_j} := \left(\frac{\partial H_{g_j}}{\partial \xi}, -\frac{\partial H_{g_j}}{\partial x} \right) \text{ the Hamiltonian vector field.}$$

Particular case:

$$(g_k) = \frac{1}{c_k^2} (\delta_{ij}), \quad k = 1, 2$$

$$V_{g_k} = \left(c_k^2 \xi, -\frac{1}{2} \nabla (c_k^2) |\xi|^2 \right)$$

Linear in c_k^2 !

Reconstruction

$$\int_0^T \frac{\partial X_{g_1}}{\partial X^0} (T - s, X_{g_2}(s, X^0)) \times \left((c_1^2 - c_2^2)\xi, -\frac{1}{2}\nabla(c_1^2 - c_2^2)|\xi|^2 \right) \Big|_{X_{g_2}(s, X^0)} dS \\ = \underbrace{X_{g_1}(T, X^0)}_{\text{data}} - X_{g_2}(T, X^0)$$

Inversion of weighted geodesic ray transform and use similar methods to U-Vasy.

The Linear Problem: General Case

The linearization of the map $g \rightarrow d_g$ leads to the question of invertability of the integration of two tensors along geodesics.

Let $f = f_{ij} dx^i \otimes dx^j$ be a symmetric 2-tensor in M . Define $f(x, \xi) = f_{ij}(x) \xi^i \xi^j$. The *ray transform* of f is

$$I_2 f(x, \xi) = \int_0^{\tau(x, \xi)} f(\varphi_t(x, \xi)) dt, \quad x \in \partial M, \xi \in S_x M,$$

where φ_t is the geodesic flow,

$$\varphi_t(x, \xi) = (\gamma(t, x, \xi), \dot{\gamma}(t, x, \xi)).$$

In coordinates

$$I_2 f(x, \xi) = \int_0^{\tau(x, \xi)} f_{ij}(\gamma(t)) \dot{\gamma}^i(t) \dot{\gamma}^j(t) dt.$$

The Linear Problem: General Case

Recall the Helmholtz decomposition of $F : \mathbb{R}^n \rightarrow \mathbb{R}^n$,

$$F = F^s + \nabla h, \quad \nabla \cdot F^s = 0.$$

Any symmetric 2-tensor f admits a *solenoidal decomposition*

$$f = f^s + dh, \quad \delta f^s = 0, \quad h|_{\partial M} = 0$$

where h is a symmetric 1-tensor, $d = \sigma \nabla$ is the inner derivative (σ is symmetrization), and $\delta = d^*$ is divergence.

By the fundamental theorem of calculus, $I_2(dh) = 0$ if $h|_{\partial M} = 0$. I_2 is said to be *s-injective* if it is injective on solenoidal tensors.

Local Result for Linearized Problem

Theorem (Stefanov-U-Vasy, 2014). Let f be a symmetric tensor field of order 2. Let $p \in \partial M$ be a **strictly convex** point. Assume that $I_2(f)(\gamma) = 0$ for all geodesics γ joining points near p . Then f is **s-injective near p** .

This is a **Helgason type** support theorem for tensor fields of order 2. The only previous result was for **real-analytic** metrics (**Krishnan**).

After this one uses **pseudolinearization** again to obtain the local boundary rigidity result.

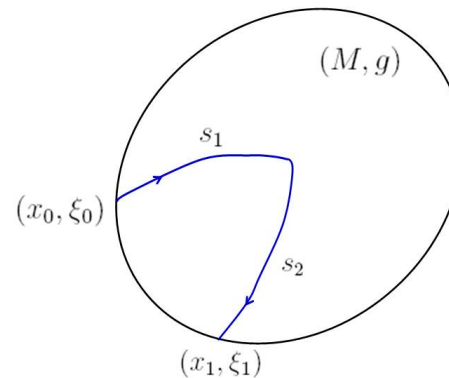
A **global** boundary rigidity result is expected to be obtained in the same way as the isotropic case assuming the **foliation condition**.

REFLECTION TRAVELTIME TOMOGRAPHY

Broken Scattering Relation

(M, g) : manifold with boundary with Riemannian metric g

$$\begin{aligned} ((x_0, \xi_0), (x_1, \xi_1), t) &\in \mathcal{B} \\ t &= s_1 + s_2 \end{aligned}$$



Theorem (Kurylev-Lassas-U)

$n \geq 3$. Then ∂M and the broken scattering relation \mathcal{B} determines (M, g) uniquely.

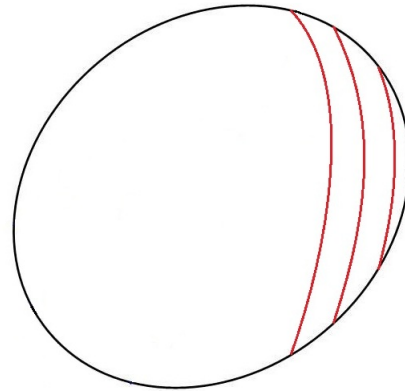
Numerical Method

(Chung-Qian-Zhao-U, IP 2011)

$$\int_0^T \frac{\partial X_{g_1}}{\partial X^0} (T - s, X_{g_2}(s, X^0)) \times \left((c_1^2 - c_2^2)\xi, -\frac{1}{2}\nabla(c_1^2 - c_2^2)|\xi|^2 \right) \Big|_{X_{g_2}(s, X^0)} dS = X_{g_1}(T, X^0) - X_{g_2}(T, X^0)$$

Adaptive method

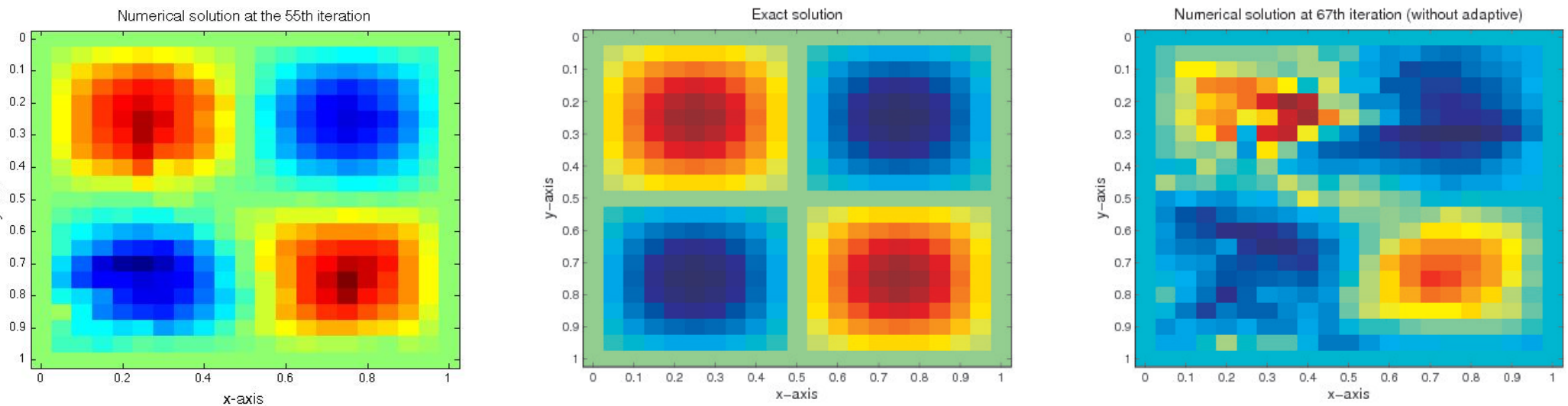
Start near $\partial\Omega$ with $c_2 = 1$ and iterate.



Numerical examples

Example 1: An example with no broken geodesics,

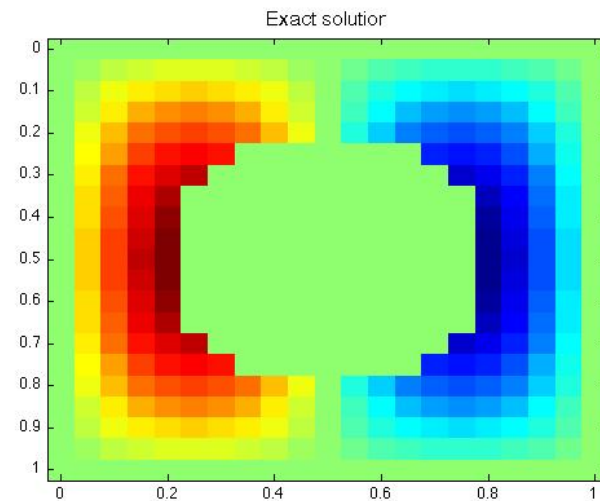
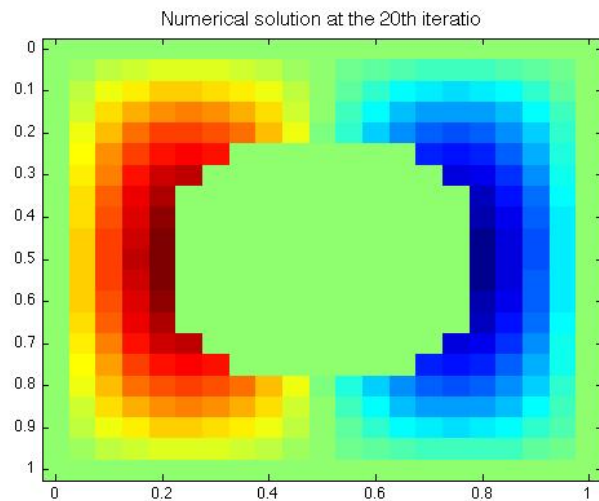
$$c(x, y) = 1 + 0.3 \sin(2\pi x) \sin(2\pi y), \quad c_0 = 0.8.$$



Left: Numerical solution (using adaptive) at the 55-th iteration. **Middle:** Exact solution. **Right:** Numerical solution (without adaptive) at the 67-th iteration.

Example 2: A known circular obstacle enclosed by a square domain. Geodesic either does not hit the inclusion or hits the inclusion (broken) once.

$$c(x, y) = 1 + 0.2 \sin(2\pi x) \sin(\pi y), \quad c_0 = 0.8.$$

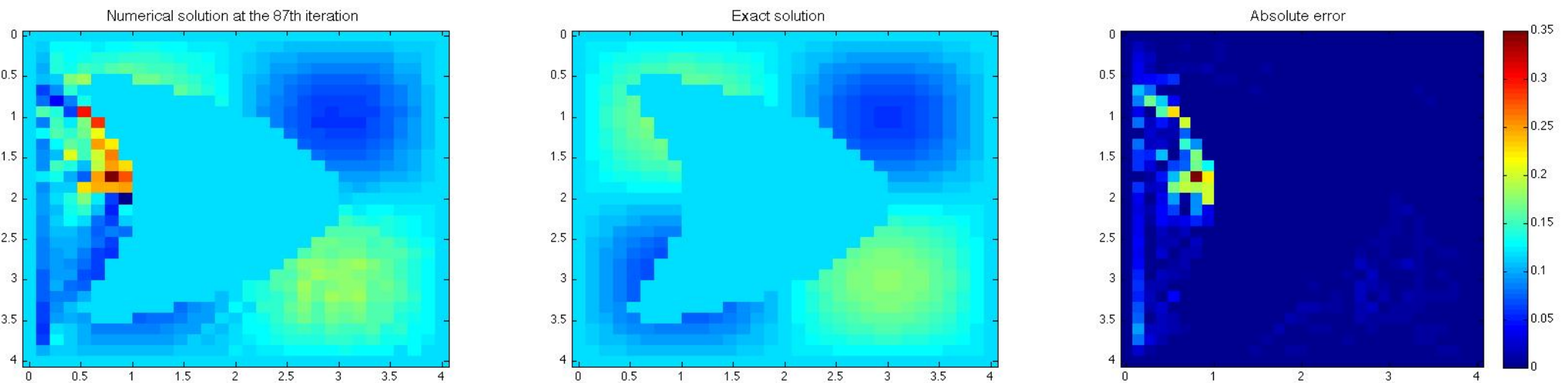


Left: Numerical solution at the 20-th iteration. The relative error is 0.094%.

Right: Exact solution.

Example 3: A concave obstacle (known).

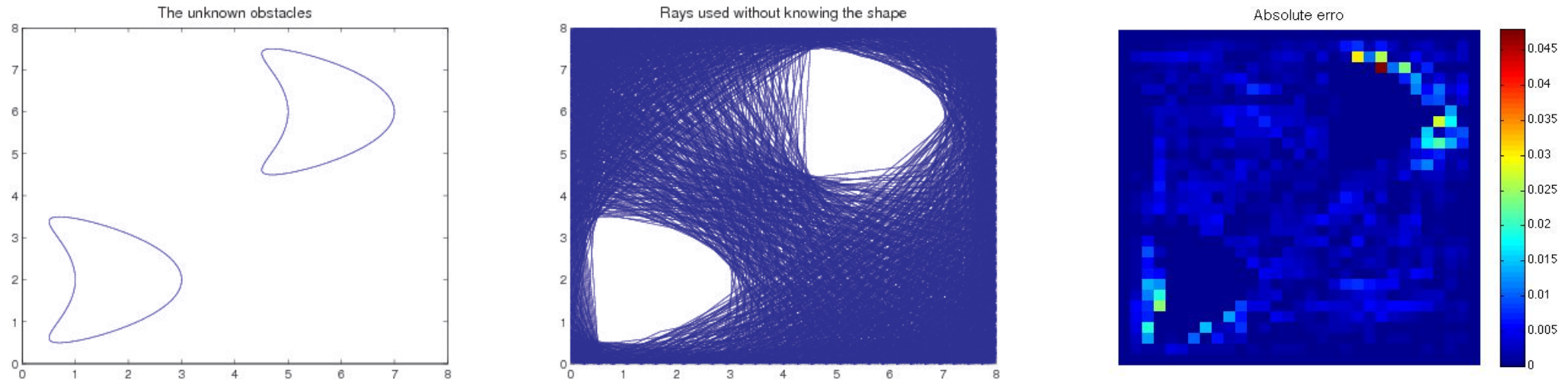
$$c(x, y) = 1 + 0.1 \sin(0.5\pi x) \sin(0.5\pi y), \quad c_0 = 0.8.$$



Left: Numerical solution at the 117-th iteration. The relative error is 2.8%.

Middle: Exact solution. **Right:** Absolute error.

Example 4: Unknown obstacles and medium.

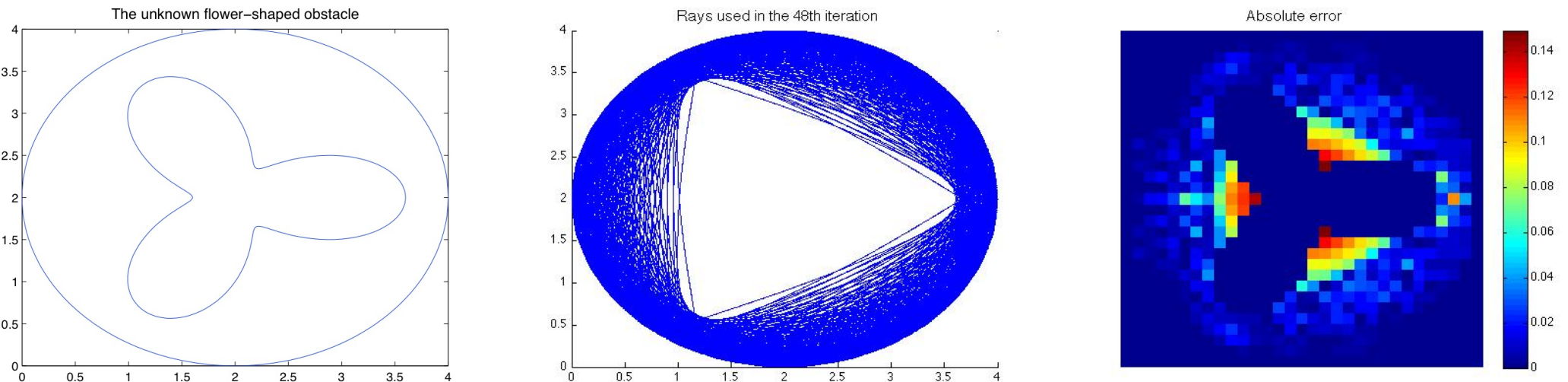


Left: The two unknown obstacles. **Middle:** Ray coverage of the unknown obstacle. **Right:** Absolute error.

Example 4: Unknown obstacles and medium (continues).

$$r = 1 + 0.6 \cos(3\theta) \text{ with } r = \sqrt{(x - 2)^2 + (y - 2)^2}.$$

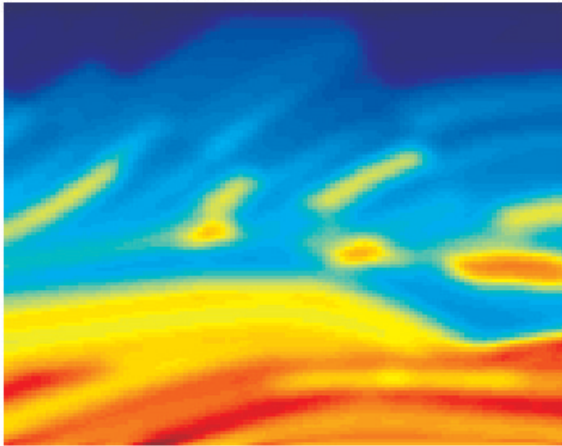
$$c(r) = 1 + 0.2 \sin r$$



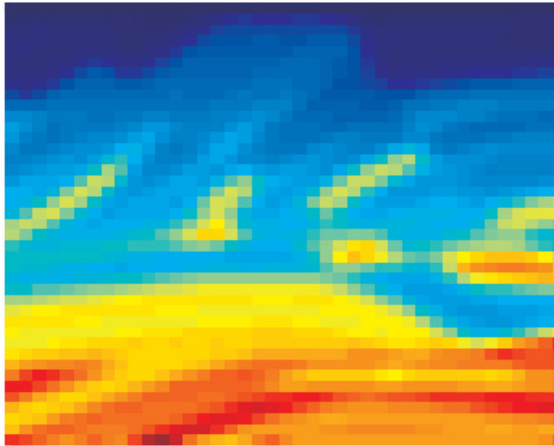
Left: The two unknown obstacles. **Middle:** Ray coverage of the unknown obstacle. **Right:** Absolute error.

Example 5: The Marmousi model.

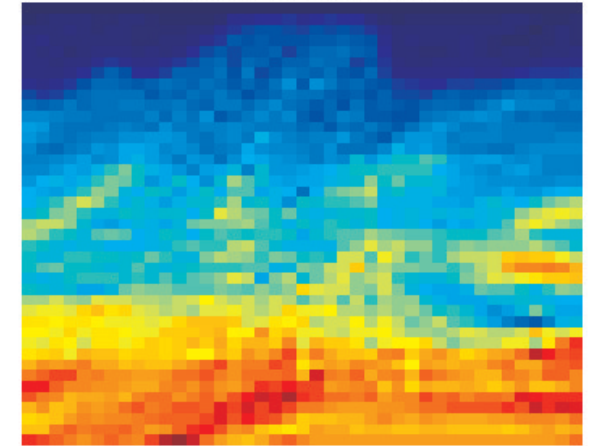
True solution on fine scale



True solution on coarse scale



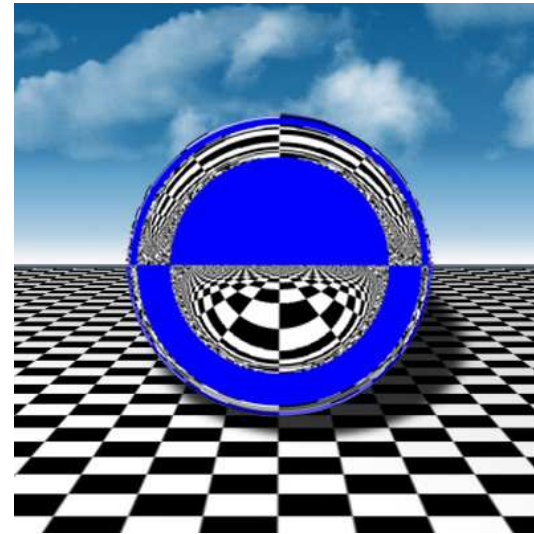
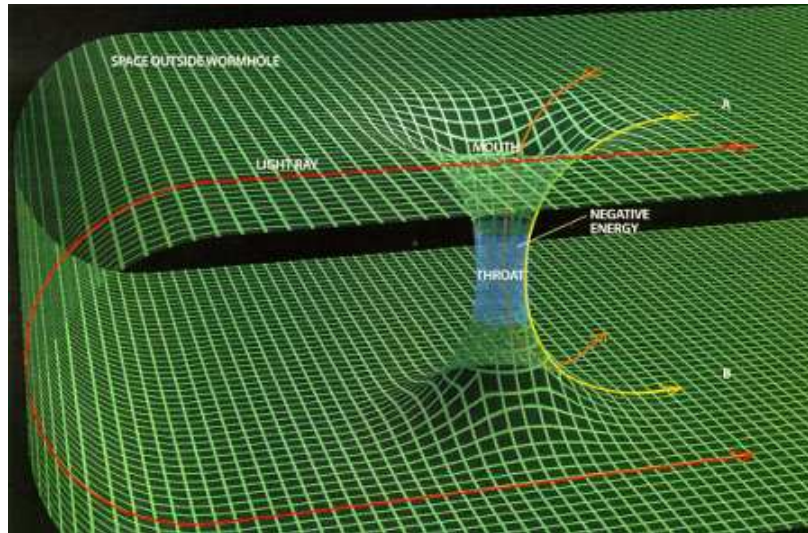
Numerical solution at the 16th iteration



Left: The exact solution on fine grid. **Middle:** The exact solution projected on a coarse grid. **Right:** The numerical solution at the 16-th iteration. The relative error is 2.24%.

Light Observation Sets

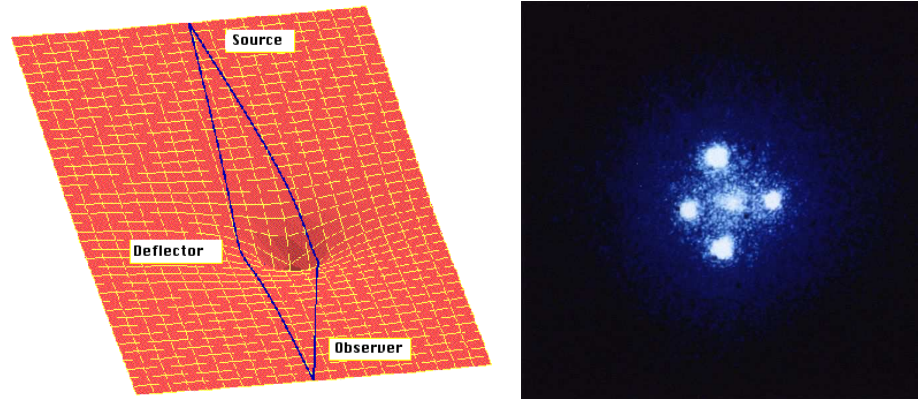
How can we determine the topology and metric of the space time?



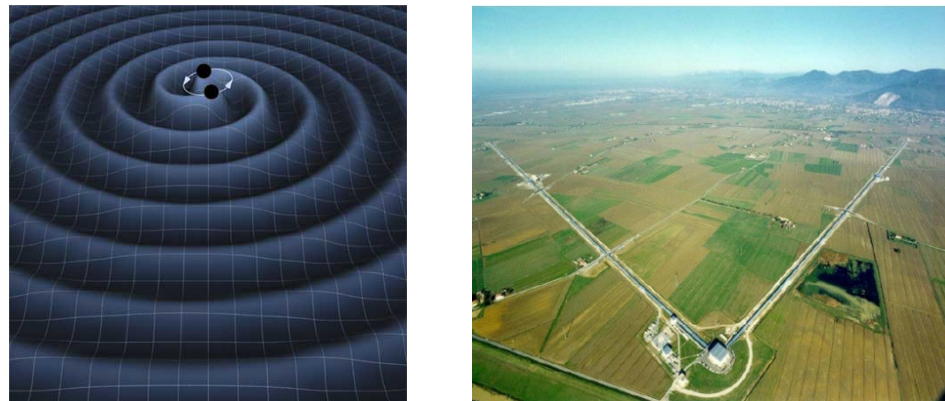
How can we determine the topology and metric of complicated structures in space-time with a radar-like device?

Figures: Anderson institute and Greenleaf-Kurylev-Lassas-U.

Passive measurements: We consider e.g. light or X-ray observations or measurements of gravitational waves.

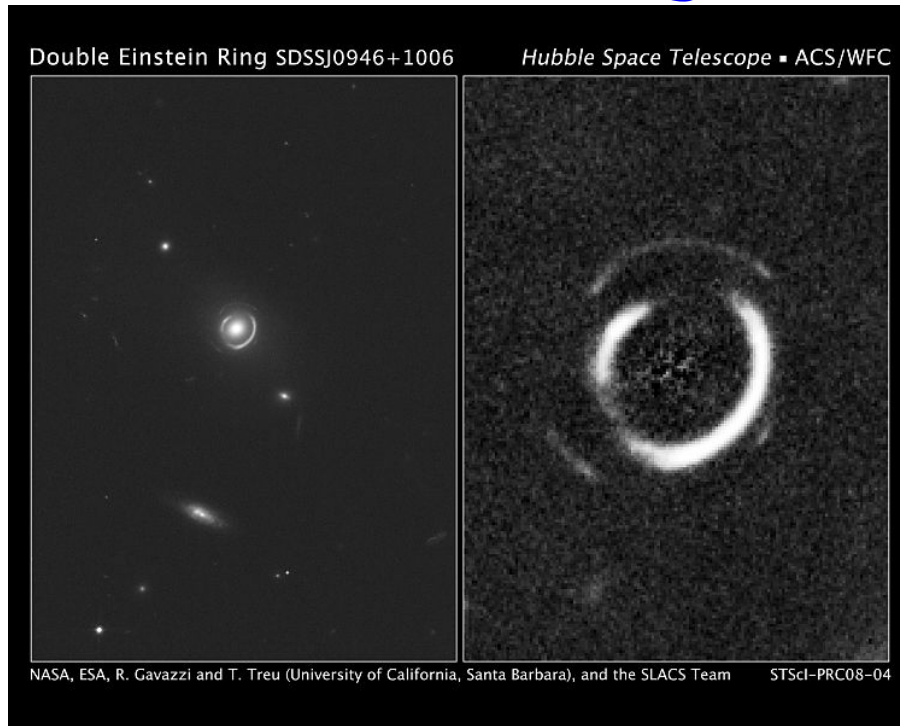


Observations from Einstein's Cross: Four images of the same distant quasar appear due to a gravitational lens.



Artistic picture on a gravitational wave and the Virgo detector.

Gravitational Lensing

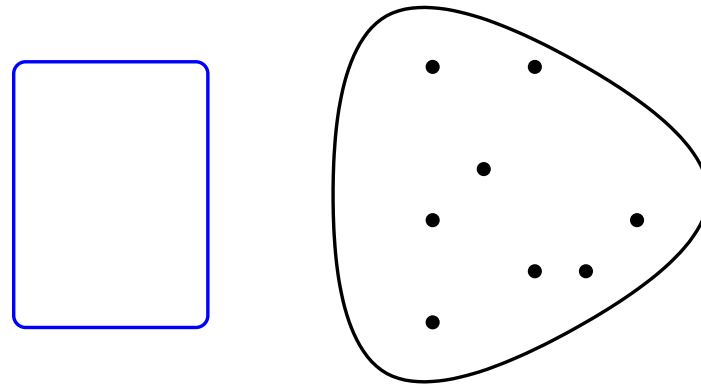


Double Einstein Ring



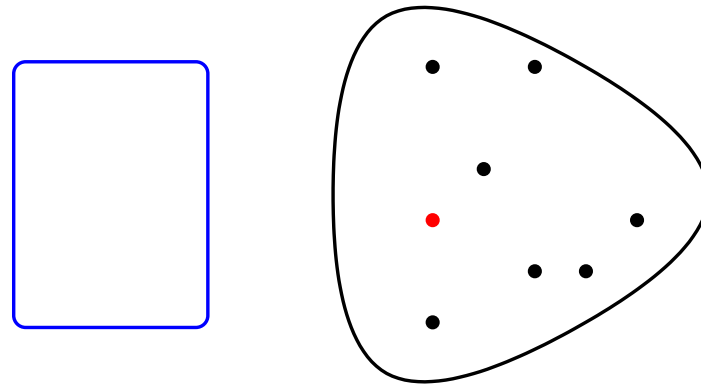
Conical Refraction

Inverse problem for passive measurements



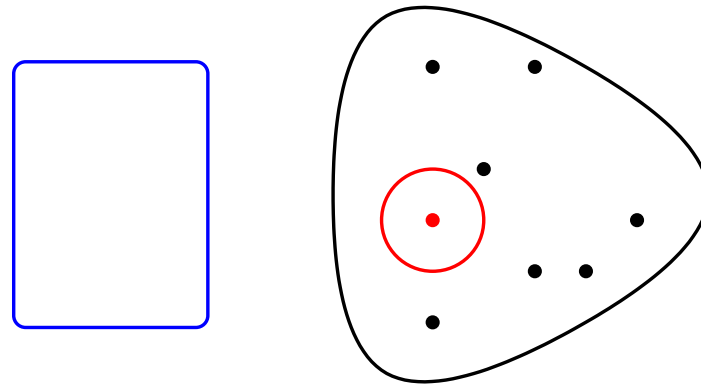
Can we determine the structure of the space-time when we observe wavefronts produced by point sources?

Inverse problem for passive measurements



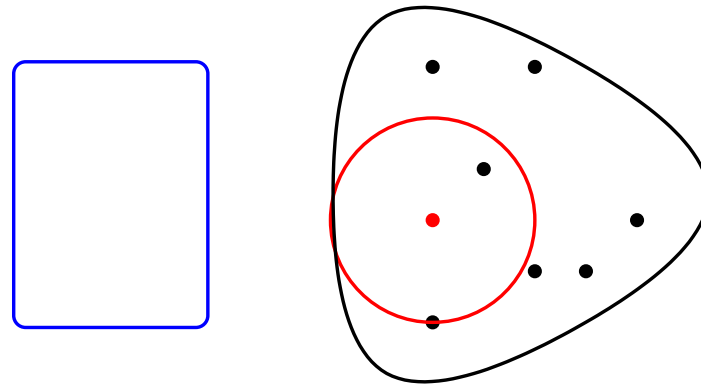
Can we determine the structure of the space-time when we observe wavefronts produced by point sources?

Inverse problem for passive measurements



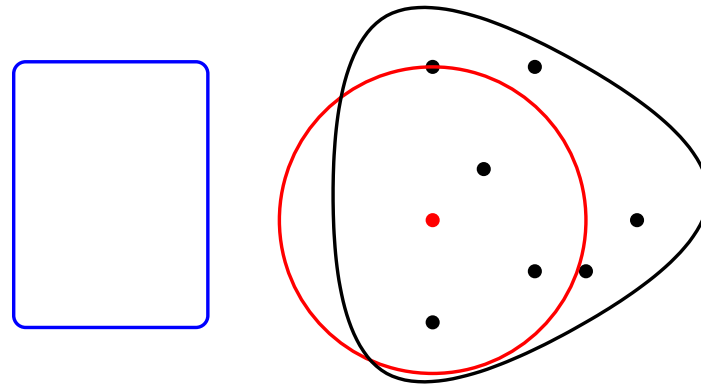
Can we determine the structure of the space-time when we observe wavefronts produced by point sources?

Inverse problem for passive measurements



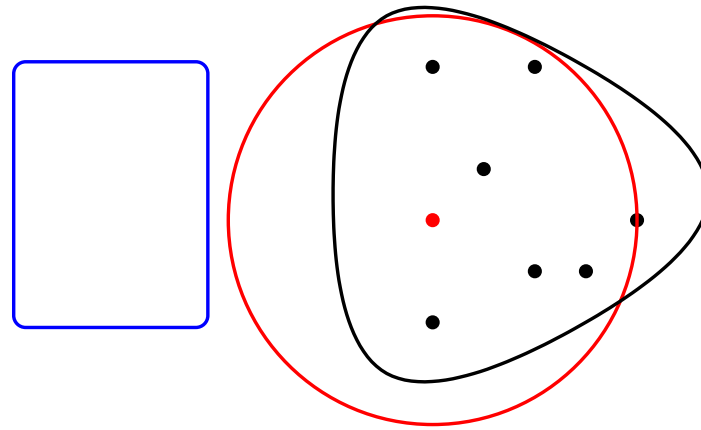
Can we determine the structure of the space-time when we observe wavefronts produced by point sources?

Inverse problem for passive measurements



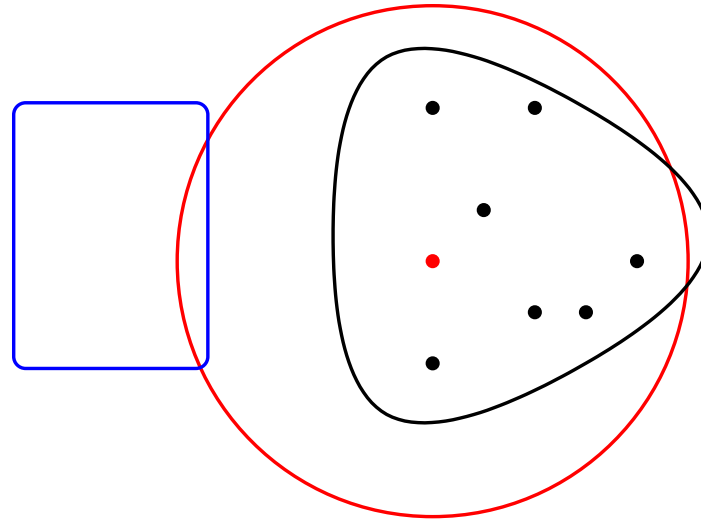
Can we determine the structure of the space-time when we observe wavefronts produced by point sources?

Inverse problem for passive measurements



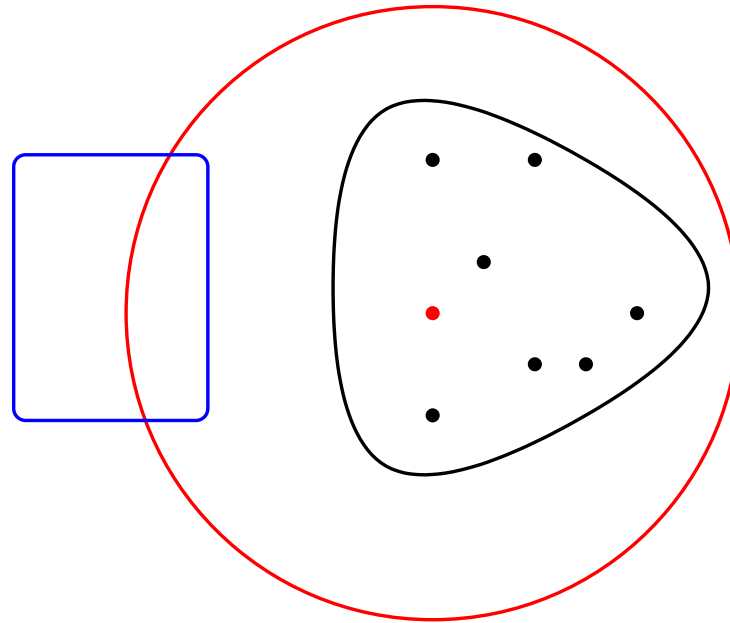
Can we determine the structure of the space-time when we observe wavefronts produced by point sources?

Inverse problem for passive measurements



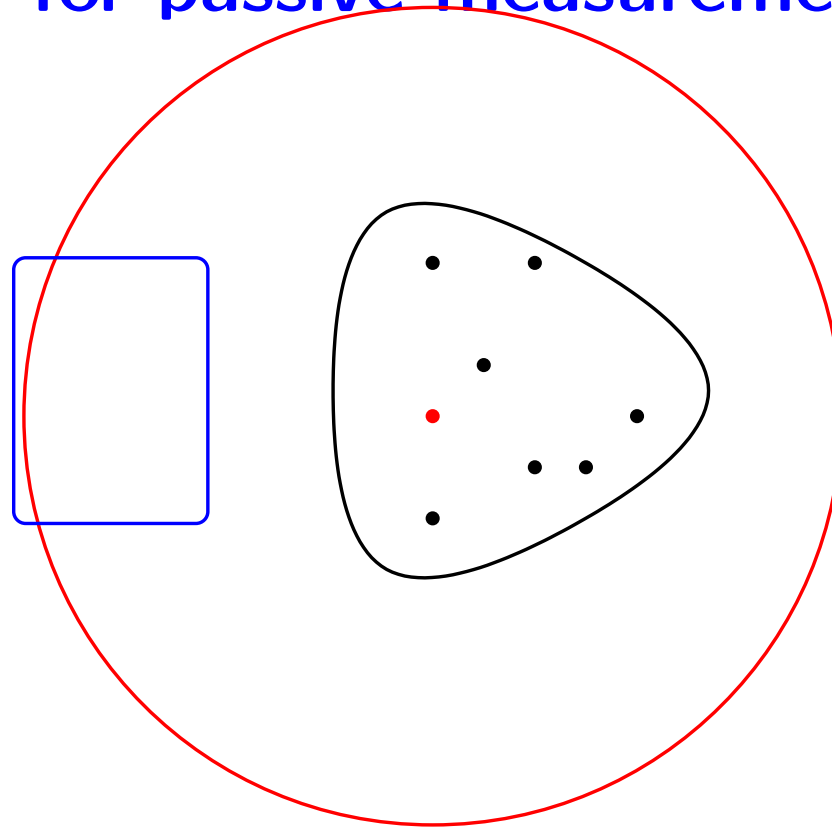
Can we determine the structure of the space-time when we observe wavefronts produced by point sources?

Inverse problem for passive measurements



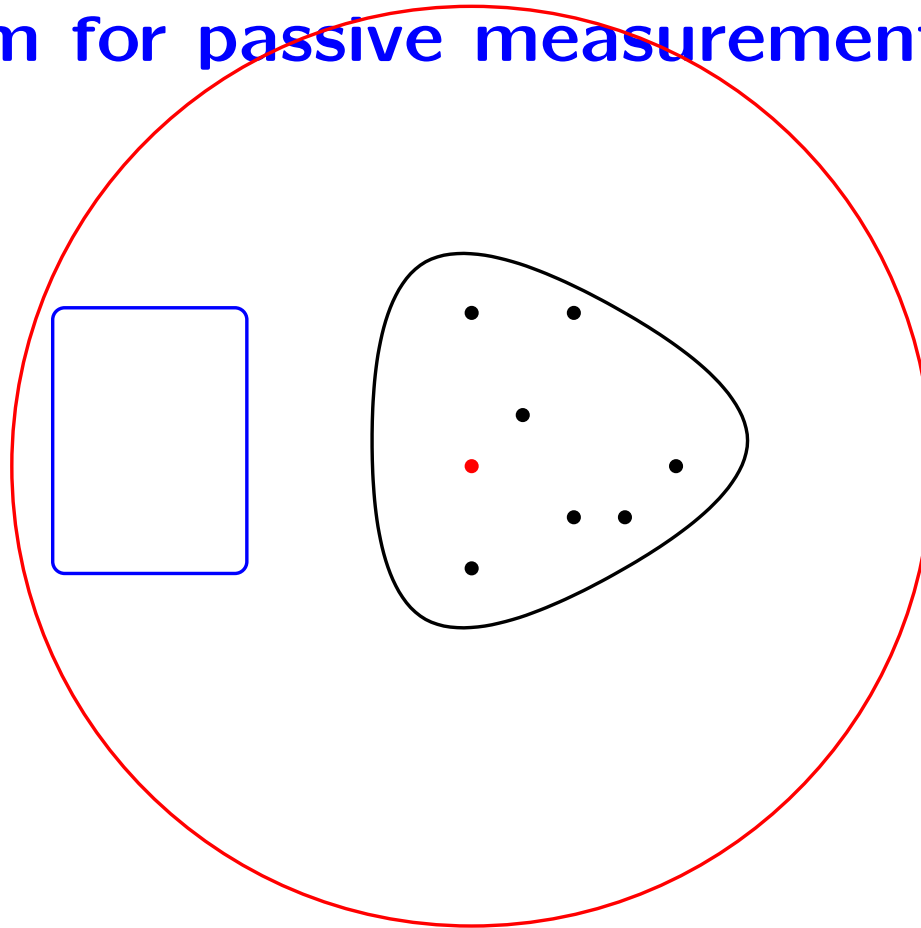
Can we determine the structure of the space-time when we observe wavefronts produced by point sources?

Inverse problem for passive measurements



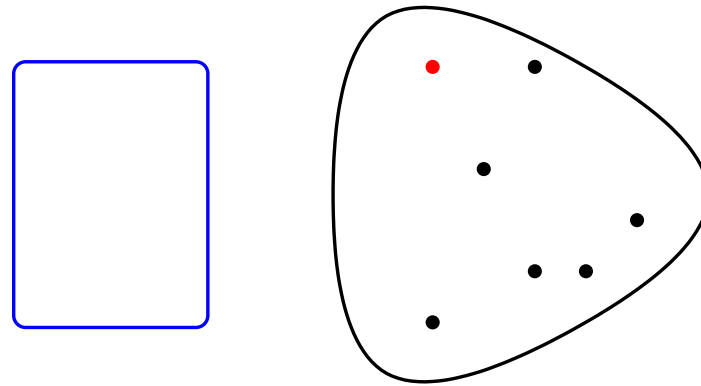
Can we determine the structure of the space-time when we observe wavefronts produced by point sources?

Inverse problem for passive measurements



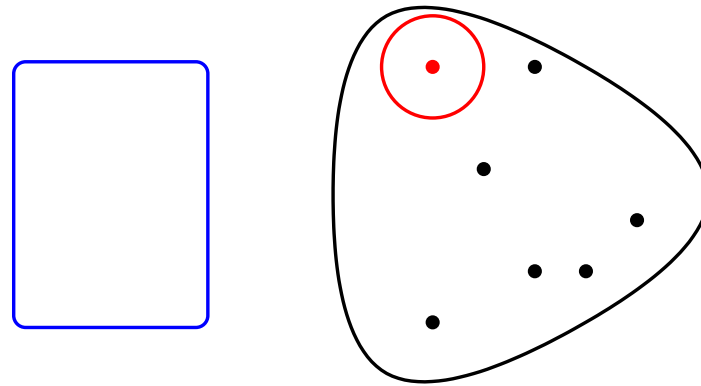
Can we determine the structure of the space-time when we observe wavefronts produced by point sources?

Inverse problem for passive measurements



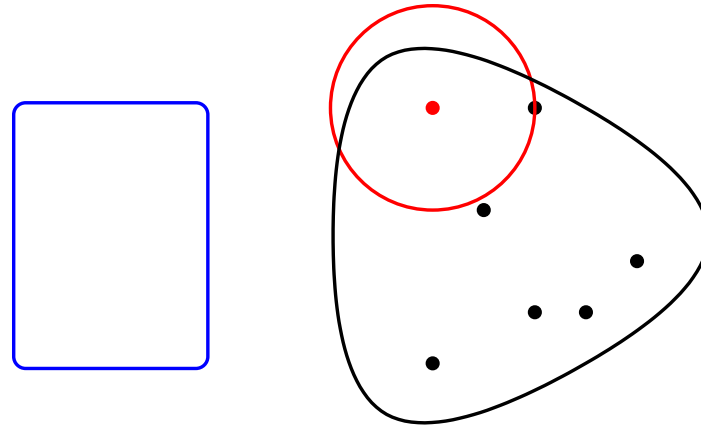
Can we determine the structure of the space-time when we observe wavefronts produced by point sources?

Inverse problem for passive measurements



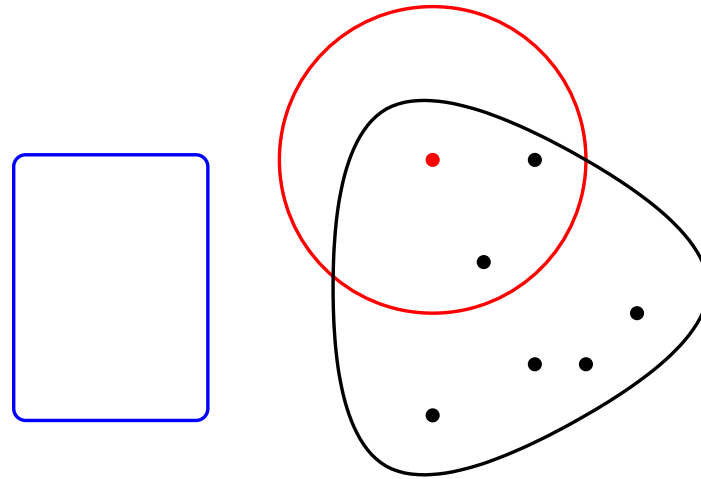
Can we determine the structure of the space-time when we observe wavefronts produced by point sources?

Inverse problem for passive measurements



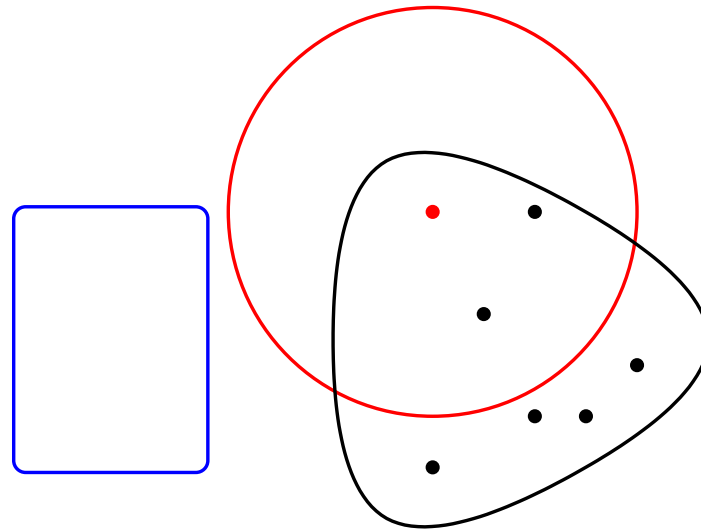
Can we determine the structure of the space-time when we observe wavefronts produced by point sources?

Inverse problem for passive measurements



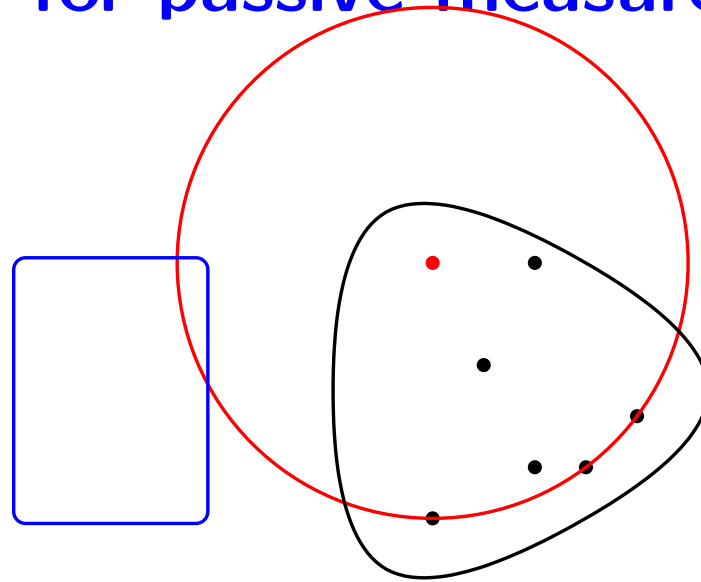
Can we determine the structure of the space-time when we observe wavefronts produced by point sources?

Inverse problem for passive measurements



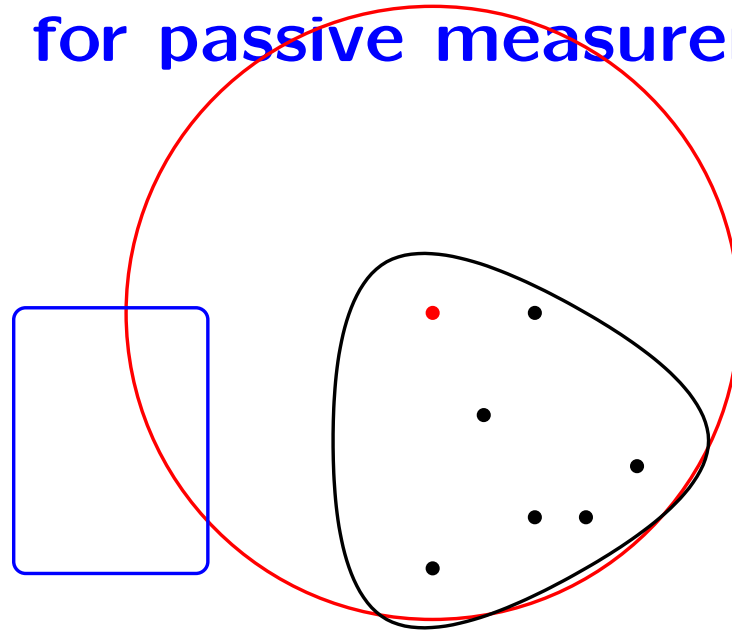
Can we determine the structure of the space-time when we observe wavefronts produced by point sources?

Inverse problem for passive measurements



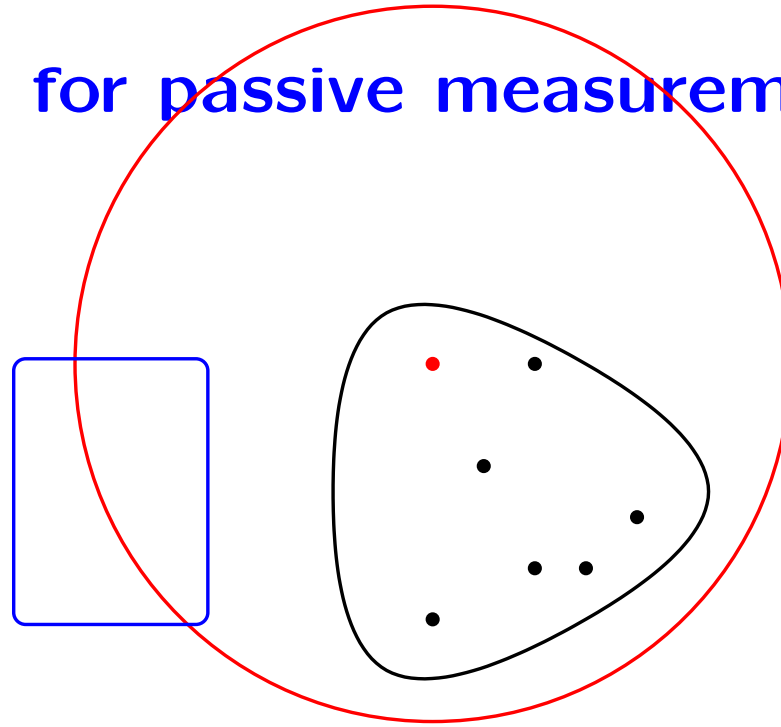
Can we determine the structure of the space-time when we observe wavefronts produced by point sources?

Inverse problem for passive measurements



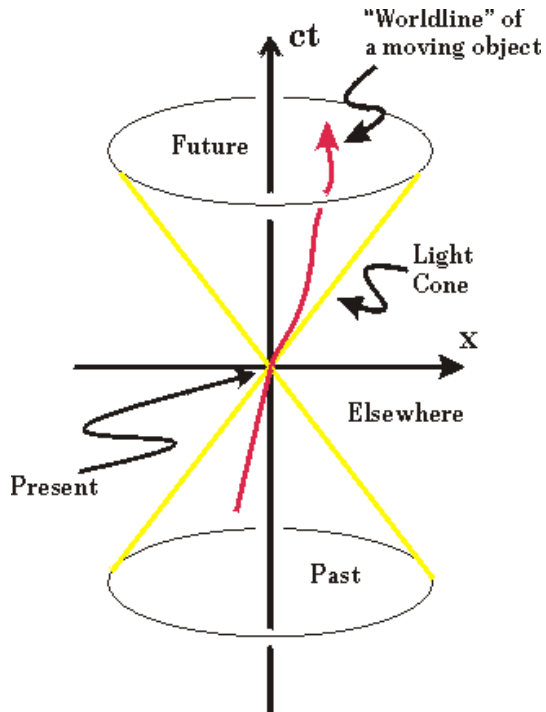
Can we determine the structure of the space-time when we observe wavefronts produced by point sources?

Inverse problem for passive measurements



Can we determine the structure of the space-time when we observe wavefronts produced by point sources?

Definitions

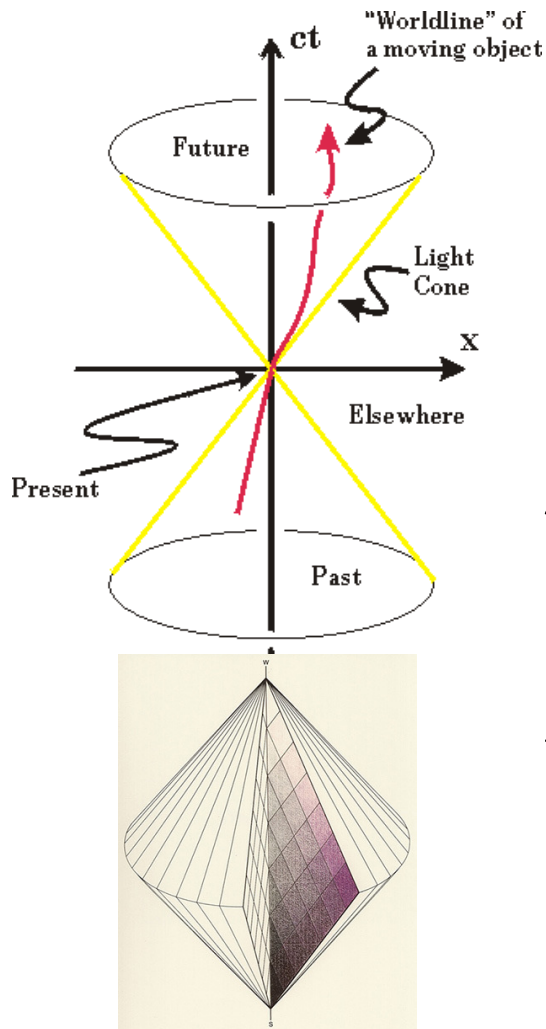


Let (M, g) be a Lorentzian manifold, where the metric g is semi-definite,
 $\xi \in T_x M$ is light-like if $g(\xi, \xi) = 0$, $\xi \neq 0$,
 $\xi \in T_x M$ is time-like if $g(\xi, \xi) < 0$,
 $\xi \in T_x M$ is causal if $g(\xi, \xi) \leq 0$,
A curve $\mu(s)$ is time-like if $\dot{\mu}(s)$ is time-like.

Example: the Minkowski metric in \mathbb{R}^4 is

$$ds^2 = -(dx^0)^2 + (dx^1)^2 + (dx^2)^2 + (dx^3)^2.$$

Definitions



Let (M, g) be a Lorentzian manifold,
 $L_q M = \{\xi \in T_q M \setminus 0; g(\xi, \xi) = 0\}$,
 $L_q^+ M \subset L_q M$ is the future light cone,
 $J^+(q) = \{x \in M; x \text{ is in causal future of } q\}$,
 $J^-(q) = \{x \in M; x \text{ is in causal past of } q\}$,
 $\gamma_{x, \xi}(t)$ is a geodesic with the initial point (x, ξ) .

(M, g) is globally hyperbolic if

there are no closed causal curves and the set
 $J^-(p_1) \cap J^+(p_2)$ is compact for all $p_1, p_2 \in M$.

Then M can be represented as $M = \mathbb{R} \times N$.

More definitions

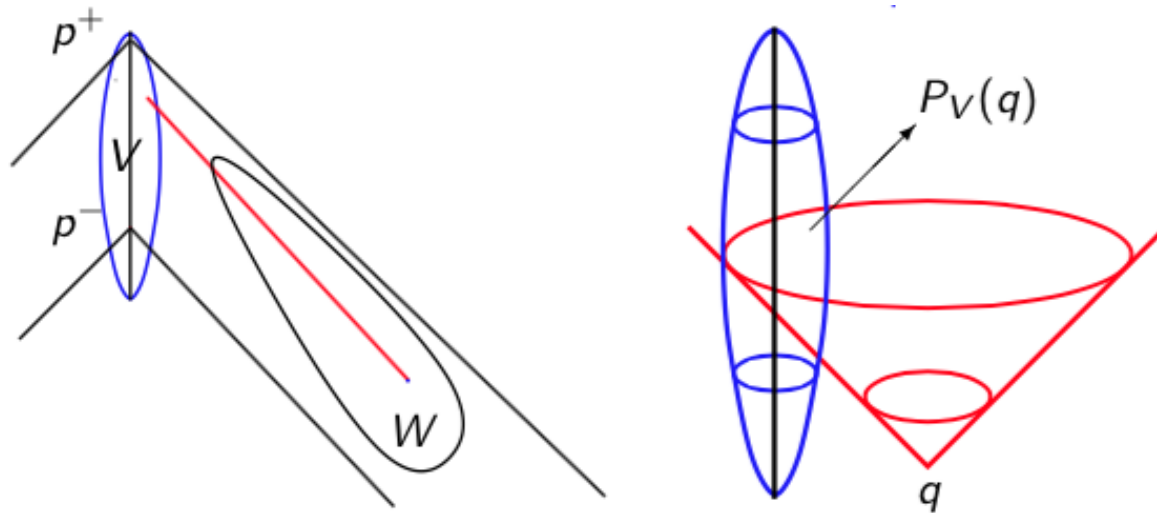
Let $\mu = \mu([-1, 1]) \subset M$ be time-like geodesics containing p^- and p^+ .

We consider observations in a neighborhood $V \subset M$ of μ .

Let $W \subset I^-(p^+) \setminus J^-(p^-)$ be relatively compact and open set.

The **light observation set** for $q \in W$ is

$$P_V(q) := \{\gamma_{q,\xi}(r) \in V; r \geq 0, \xi \in L_q^+ M\}.$$

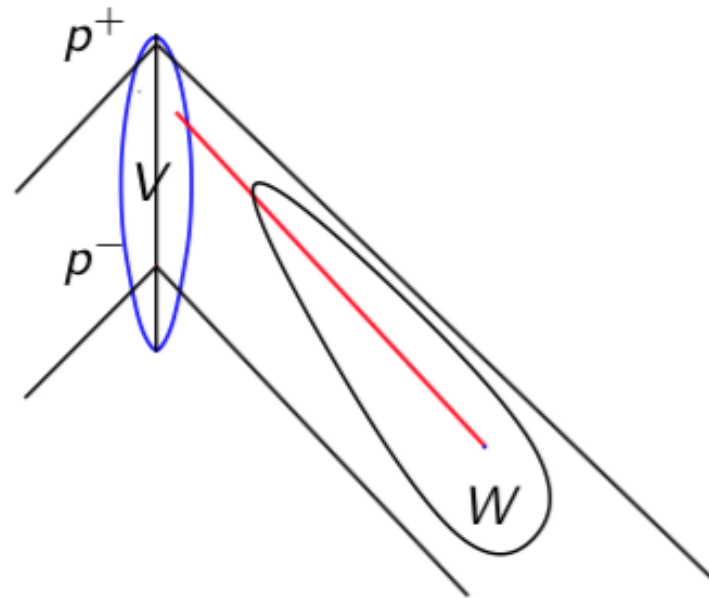


Theorem (Kurylev-Lassas-U, 2013). Let (M, g) be an open, globally hyperbolic Lorentzian manifold of dimension $n \geq 3$. Assume $\mu \subset V$ is a time-like geodesic containing the points p^- and p^+ , and $V \subset M$ is a neighborhood of μ .

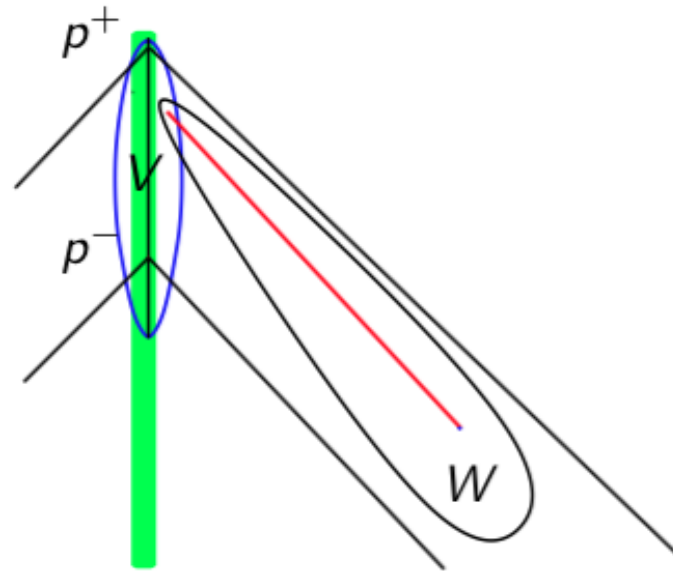
Let $W \subset I^-(p^+) \setminus J^-(p^-) \subset M$ be a relatively compact open set. The set V and the collection of sets

$$P_V(q) \subset V, \text{ where } q \in W$$

determine the **conformal type** of the set (W, g) .



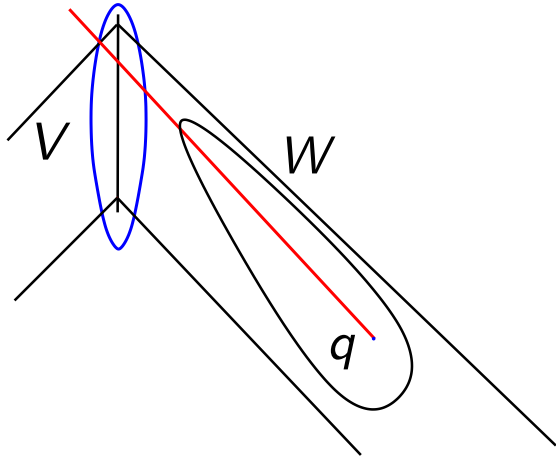
Reconstruction of conformal factor in vacuum



Assume that we are given $(V, g|_V)$.

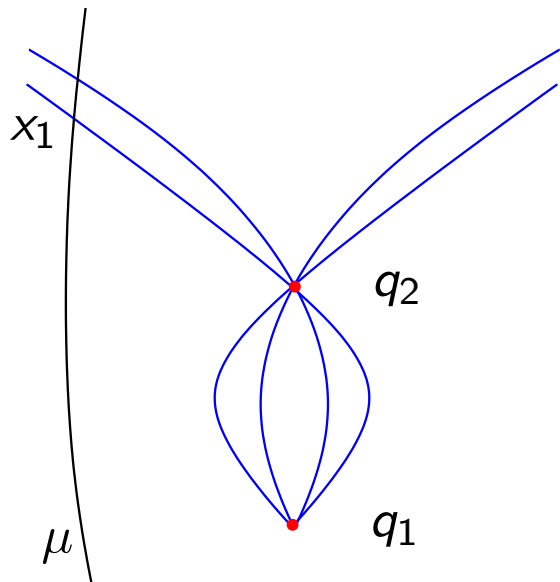
When $x \in W$ can be connected to observation set V with a light-like geodesic $\gamma \subset W$ that lies in vacuum, we can find the conformal factor and thus the metric tensor g near x .

Reconstruction of the topological structure of W

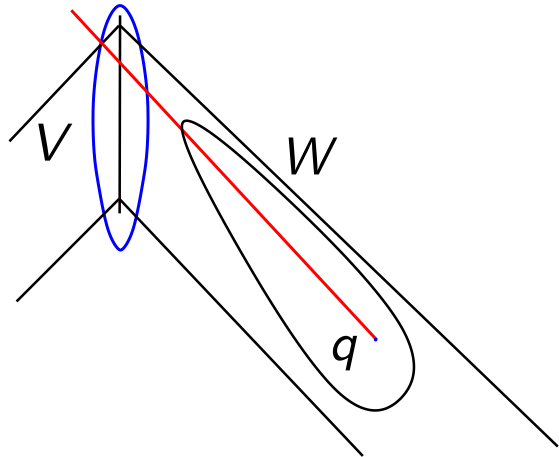


Assume that $q_1, q_2 \in W$ are such that $P_V(q_1) = P_V(q_2)$. Then all light-like geodesics from q_1 to V go through q_2 .

Let x_1 be the earliest point of $\mu \cap P_V(q_1)$.

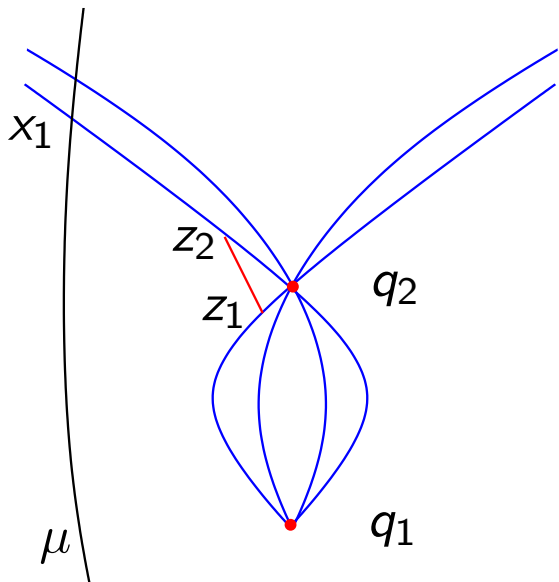


Reconstruction of the topological structure of W

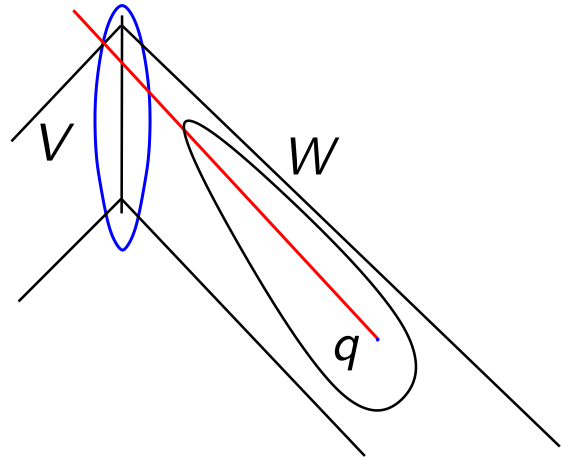


Assume that $q_1, q_2 \in W$ are such that $P_V(q_1) = P_V(q_2)$. Then all light-like geodesics from q_1 to V go through q_2 .

Let x_1 be the earliest point of $\mu \cap P_V(q_1)$. Using a short cut argument we see that there is a causal curve from q_1 to x_1 that is not a geodesic.



Reconstruction of the topological structure of W



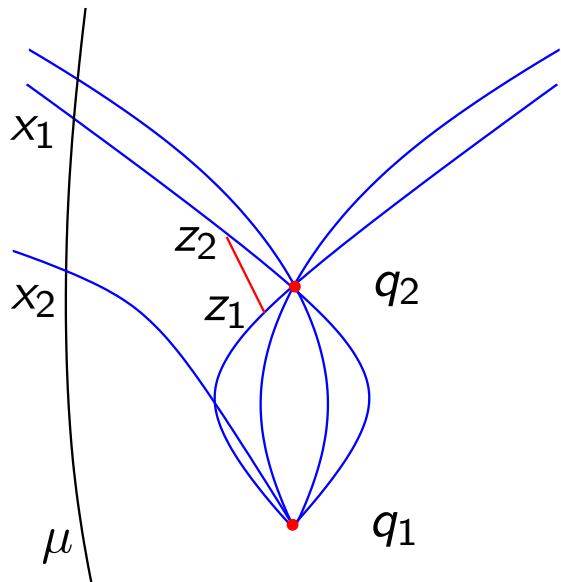
Assume that $q_1, q_2 \in W$ are such that $P_V(q_1) = P_V(q_2)$. Then all light-like geodesics from q_1 to V go through q_2 .

Let x_1 be the earliest point of $\mu \cap P_V(q_1)$. Using a short cut argument we see that there is a causal curve from q_1 to x_1 that is not a geodesic.

This implies that q_1 can be observed on μ before x_1 .

The map $P_V : q \mapsto 2^{TV}$ is continuous and one-to-one.

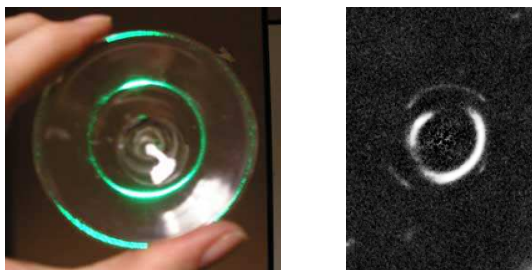
As \overline{W} is compact, the map $P_V : \overline{W} \rightarrow P_V(\overline{W})$ is a homeomorphism.



Determination of conformal type

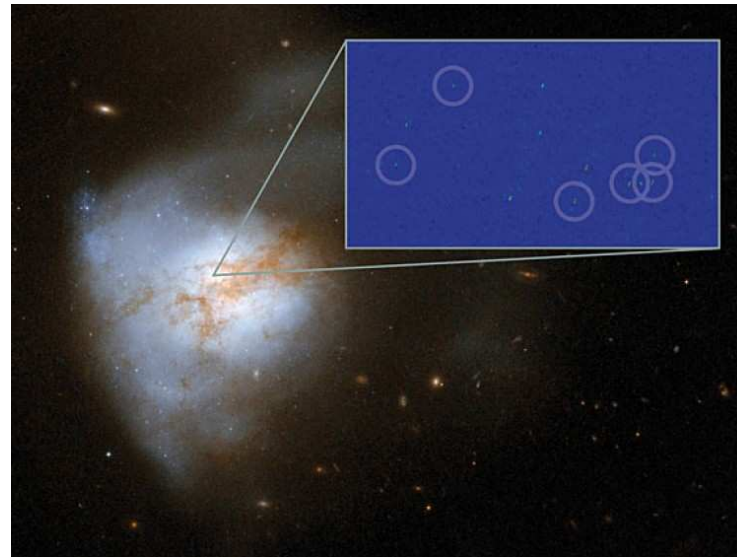
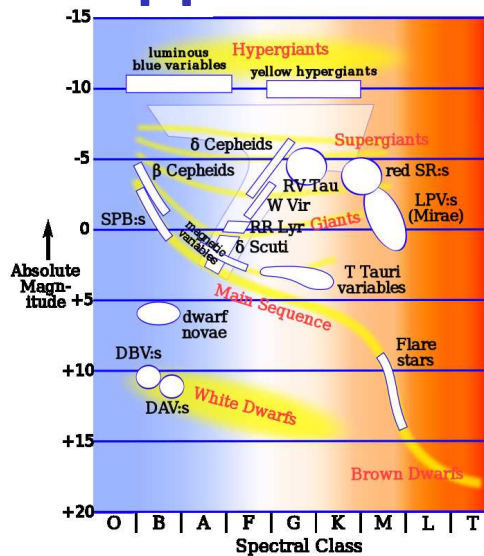
The light cone $L_x^+M \subset T_xM$ is a quadratic variety and thus real-analytic. When we are given an open subset of it, the whole surface can be determined. This determines the conformal type of the metric g at any $x \in U$.

Due to caustics, there are many exceptional cases.

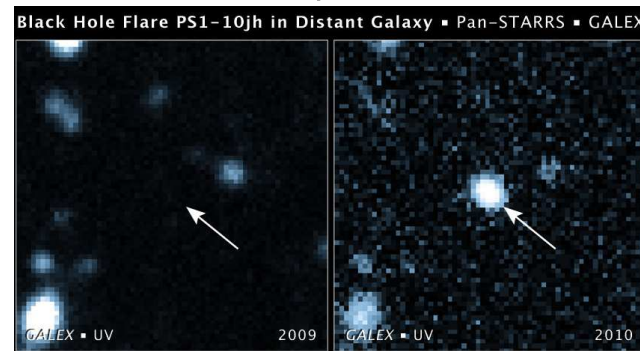
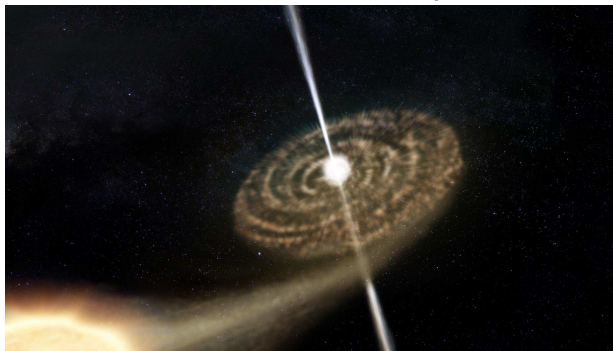


Figures: Wineglass by P. Doherty and Einstein's ring by R. Gavazzi and T. Treu.

Possible applications of the theorem



Left: Variable stars in Hertzsprung-Russell diagram on star types.
 Right: Galaxy Arp 220 (Hubble Space Telescope)



Artistic impressions on matter falling into a black hole and
 Pan-STARRS1 telescope picture.